General Disclaimer

One or more of the Following Statements may affect this Document

- This document has been reproduced from the best copy furnished by the organizational source. It is being released in the interest of making available as much information as possible.

- This document may contain data, which exceeds the sheet parameters. It was furnished in this condition by the organizational source and is the best copy available.

- This document may contain tone-on-tone or color graphs, charts and/or pictures, which have been reproduced in black and white.

- This document is paginated as submitted by the original source.

- Portions of this document are not fully legible due to the historical nature of some of the material. However, it is the best reproduction available from the original submission.

Produced by the NASA Center for Aerospace Information (CASI)

Semiannual Report for

NUMERICAL METHODS FOR ANALYZING ELECTROMAGNETIC SCATTERING

September 25, 1984 to March 24, 1985

Submitted to

Dr. Y. C. Cho

National Aeronautics and Space Administration
Lewis Research Center (MS 54-3)
Cleveland, OH 44113

(NASA-CR-175507) NUMERICAL METHODS FOR ANALYZING ELECTROMAGNETIC SCATTERING Semiannual Report, 25 Sep. 1984 - 24 Mar. 1985 (Illinois Univ.) 66 p HC A04/MF A01 CSCL 20N G3/32

N85-21438

Unclas 14473

Grant No. NAG-3-475

Prepared by

S. W. Lee, Y. T. Lo, S. L. Chuang, and C. S. Lee

Electromagnetics Laboratory
Department of Electrical and Computer Engineering
University of Illinois
Urbana, IL 61801

March 24, 1985

Semiannual Report for

NUMERICAL METHODS FOR ANALYZING ELECTROMAGNETIC SCATTERING

September 25, 1984 to March 24, 1985

Submitted to

Dr. Y. C. Cho

National Aeronautics and Space Administration
Lewis Research Center (MS 54-3)
Cleveland, OH 44113

Grant No. NAG-3-475

Prepared by

S. W. Lee, Y. T. Lo, S. L. Chuang, and C. S. Lee

Electromagnetics Laboratory
Department of Electrical and Computer Engineering
University of Illinois
Urbana, IL 61801

March 24, 1985

TABLE OF CONTENTS

Page

I. INTRODUCTION. 1

II. TECHNICAL PERSONNEL 1

III. PRESENTATION AND PUBLICATIONS 1

IV. TECHNICAL PROGRESS. 2

(1) Analysis of the normal modes in a waveguide coated with lossy material 3

(2) The RCS calculation. 22
(3) A by-product of our research: a waveguide coated with a very lossy magnetic material 47
(4) Conclusions and future prospects 54

REFERENCES. 57

LIST OF TABLES

TABLE		Page
1.	MODAL SEPARATION IN AN OVERMODED WAVEGUIDE COATED WITH A LOSSY MATERIAL.	17
2.	ATTENUATION CONSTANTS OF THE NORMAL MODES IN A CIRCULAR WAVEGUIDE COATED WITH A LOSSY MATERIAL (CROWLOY BX113, $\varepsilon_r = 12 - j0.144$, $\mu_r = 1.74 - j3.306$) FOR 0.6% ($a = 3.95$ cm, $\tau = 0.025$ cm) AND 1.3% ($a = 3.95$ cm, $\tau = 0.05$ cm) COATINGS.	38
3.	ATTENUATION CONSTANTS OF THE NORMAL MODES IN A CIRCULAR WAVEGUIDE COATED WITH A LOSSY MATERIAL (POLY-2,5-DICHLOROSTYRENE, $\varepsilon_r = 7.3$, $\mu_r = 9.1 - j0.32$) FOR 1% ($a = 10$ cm, $\tau = 0.1$ cm) AND 3% ($a = 10$ cm, $\tau = 0.3$ cm) COATINGS.	42

LIST OF FIGURES

Figure		Page
1.	Attenuation constants as a function of frequency for both magnetic ($\varepsilon_r = 1$, $\mu_r = 1.5 - j2$) and dielectric coatings ($\mu_r = 1$, $\varepsilon_r = 1.5 - j2$).	4
2.	Radial wave numbers of the normal modes in a waveguide coated with a lossless dielectric material ($\mu_r = 1$, $\varepsilon_r = 10$)	6
3.	Radial wave numbers of the normal modes in a waveguide coated with a lossless magnetic material ($\varepsilon_r = 1$, $\mu_r = 10$)	7
4.	Radial wave numbers of the normal modes in a circular waveguide coated with a lossy dielectric material ($\mu_r = 1$, $\varepsilon_r = 10e^{-j\phi}$, $\phi = 5°$).	8
5.	Radial wave numbers of the normal modes in a circular waveguide coated with a lossy magnetic material ($\varepsilon_r = 1$, $\mu_r = 10^{-j\phi}$, $\phi = 5°$)	9
6.	Attenuation constants of the normal modes coated with a lossy dielectric material ($\mu_r = 1$, $\varepsilon_r = 10e^{-j\phi}$, $\phi = 5°$). . . .	10
7.	Attenuation constants of the normal modes coated with a lossy magnetic material ($\varepsilon_r = 1$, $\mu_r = e^{-j\phi}$, $\phi = 5°$).	11
8.	Radial wave numbers of the normal modes in a waveguide coated with a lossy dielectric material ($\mu_r = 1$, $\varepsilon_r = 10e^{-j\phi}$, $\phi = 45°$)	13
9.	Radial wave numbers of the normal modes in a waveguide coated with a lossy magnetic material ($\varepsilon_r = 1$, $\mu_r = 10e^{-j\phi}$, $\phi = 45°$).	14
10.	Attenuation constants of the normal modes in a waveguide coated with a lossy dielectric material ($\mu_r = 1$, $\varepsilon_r = 10e^{-j\phi}$, $\phi = 45°$).	15
11.	Attenuation constants of the normal modes in a waveguide coated with a lossy magnetic material ($\varepsilon_r = 1$, $\mu_r = 10e^{-j\phi}$, $\phi = 45°$).	16
12.	Radial wave numbers of the normal modes in a waveguide coated with a lossy magnetic material (expanded version of Figure 9) ($\varepsilon_r = 1$, $\mu_r = 10e^{-j\phi}$, $\phi = 45°$).	20
13.	Radial wave numbers of the normal modes in a waveguide coated with a lossy magnetic material ($\varepsilon_r = 1$, $\mu_r = 10e^{-j\phi}$, $\phi = 60°$).	21

Figure		Page
14.	A PEC-terminated cylindrical waveguide coated with a lossy material is illuminated by an incident plane wave. . . .	23
15.	The power of the TE_{11} mode transmitted to a circular waveguide from a normally incident plane wave using the Kirchhoff method and Wiener Hopf technique [10].	24
16.	The diffracted field on the plane of the waveguide opening . .	26
17.	The approximate dimensions of the jet inlets of the three military aircrafts (B-1B, F-15C and F-5E) in terms of the free-space wavelength (Source: Jane's World of Airplane, 83/84)	27
18.	The RCS's from the interior irradiation and the rim diffraction [11] of a circular waveguide terminated by a PEC as a function of the incident angle (a/λ = 1.2, length = 26.46 cm, a = 3.95 cm, vertical polarization)	29
19.	The RCS's from the interior irradiation and the rim diffraction [12] of a circular waveguide terminated by a PEC as a function of the incident angle (a/λ = 2.3, length 37.8 cm, a = 7.56 cm, vertical polarization).	30
20.	The RCS's from the interior irradiation of the TE_{11} mode only and the rim diffraction of a circular waveguide terminated by a PEC for a normal incidence as a function of a/λ (Source: Johnson and Moffatt, 1980 [10])	31
21.	The RCS from a circular waveguide terminated by a PEC in comparison with other solutions as a function of incident angle (a/λ = 1.2, length = 26.46 cm, a = 3.95 cm, vertical polarization)	32
22.	The total RCS and the RCS's from a few low-order modes in a circular waveguide terminated by a PEC (a/λ = 1.2, length = 26.46 cm, a = 3.95 cm, vertical polarizaton).	34
23.	(a) The circular waveguide coated with a lossy material with a taper near the waveguide mouth. (b) The approximation of (a) in the calculation of the RCS in this report with an assumption that all normal modes are transmitted without reflection or modal conversion	36
24.	Power intensity of the HE_{11} mode as a function of the radial distance in a waveguide coated with a lossy material (Crowloy BX113, ε_r = 12 - j0.144, μ_r = 1.74 - j3.306) with a total power of 1 watt: f = 9.2 GHz, a = 3.95 cm, A. b = 3.95 cm (τ = 0 cm), B. b = 3.975 cm (τ = 0.025 cm), and C. b = 4.00 cm (τ = 0.05 cm).	37

Figure | Page

25. The RCS's as a function of the incident angle from a circular waveguide coated with a lossy material (Crowloy BX113, $\varepsilon_r = 12 - j0.144$, $\mu_r = 1.74 - j3.306$) and terminated by a PEC for layer thicknesses of $\tau = 0$, 0.025 cm (0.6% coating) and 0.05 cm (1.3% coating) ($a = 3.95$ cm, $f = 9.2$ GHz, $a/\lambda = 1.2$, length = 26.46 cm, vertical polarization) 40

26. Power intensity of the HE_{11} mode as a function of the radial distance in a waveguide coated with a lossy material (Poly-2,5-dichlorostyrene, $\varepsilon_r = 7.3$, $\mu_r = 9.1 - j0.32$) with a total power of 1 watt: $f = 10$ GHz, $a = 10$ cm, A. $b = 10$ cm ($\tau = 0$ cm), B. $b = 10.1$ cm ($\tau = 0.1$ cm), and C. 10.3 cm ($\tau = 0.3$ cm) 41

27. The RCS's as a function of the incident angle from a circular waveguide coated with a lossy material (poly-2,5-dichlorostyrene, $\varepsilon_r = 7.3$, $\mu_r = 9.1 - j0.32$) and terminated by a PEC for layer thicknesses of $\tau = 0$, 0.1 cm (1% coating) and 0.3 cm (3% coating) ($a = 10$ cm, $f = 10$ GHz, $a/\lambda = 3.33$, length = 60 cm, vertical polarization) . 44

28. Power intensity of the HE_{11} mode as a function of the radial distance in a waveguide coated with a lossy material (poly-2,5-dichlorostyrene, $\varepsilon_r = 7.3$, $\mu_r = 9.1 - j0.32$) with a total power of 1 watt: $f = 10$ GHz, $a = 40$ cm, A. $b = 40$ ($\tau = 0$ cm), B. $b = 40.1$ cm ($\tau = 0.1$ cm), and C. $b = 40.2$ cm ($\tau = 0.2$ cm) 45

29. The RCS's as a function of the layer thickness from a circular waveguide coated with a lossy material (poly-2,5-dichlorostyrene, $\varepsilon_r = 7.3$, $\mu_r = 9.1 - j0.32$) and terminated by a PEC ($a = 40$ cm, $f = 10$ GHz, $a/\lambda = 13.3$, length = 240 cm, vertical polarization). 46

30. The magnitudes of the angular electric and magnetic fields of the HE_{11} mode at the interface between the air and the lossy material relative to those at the center of the waveguide as a function of the inner radius of the waveguide, $a(\tau = 0.1$ cm). 48

31. The attenuation of the HE_{11} mode as a function of the inner radius of the waveguide, a ($\tau = 0.1$ cm). 49

32. (a) The far-field radiation patterns of the HE_{11} mode in a coated guide: $a = 10$ cm, $b = 10.1$ cm, $a/\lambda = 6.67$. Loss = 2.84×10^{-2}.
(b) The far-field radiation patterns of the TE_{11} mode in an empty guide: $a = b = 10$ cm, $a/\lambda = 6.67$ 51

Figure | Page

33. The far-field radiation patterns of the HE_{11} mode in a coated guide: a = 5 cm, b = 5.1 cm, $a/\lambda = 3.33$. Loss = 2.28×10^{-1} dB/m. 52

34. The far-field radiation patterns of the HE_{11} mode in a coated guide: a = 2 cm, b = 2.1 cm, $a/\lambda = 1.33$. Loss = 3.72 dB/m 53

I. INTRODUCTION

The research grant NAG 3-475 entitled "Numerical Methods for Analyzing Electromagnetic Scattering" was awarded to the Univeristy of Illinois by NASA-Lewis Research Center on September 28, 1983. Dr. Y. C. Cho of NASA's Microwave Amplifier Section is the Technical Officer, and Mr. Boyd M. Bane is the contracting officer. The total amount of funds received by the University is

$$\$74,985 + \$80,009 = \$154,994$$

to cover the period from

September 25, 1983 to November 25, 1985 (26 months).

This report is the third semiannual report which covers the period September 25, 1984 to March 24, 1985.

II. TECHNICAL PERSONNEL

S. W. Lee	Professor of Electrical and Computer Engineering
Y. T. Lo	Professor of Electrical and Computer Engineering
S. L. Chuang	Assistant Professor of Electrical and Computer Engineering
C. S. Lee	Research Assistant of the Department of Electrical and Computer Engineering

III. PRESENTATION AND PUBLICATIONS

1. Professors S. W. Lee and Y. T. Lo traveled to NASA Lewis on February 24, 1985 to present a talk entitled "Scattering from Circular Guide Coated with Lossy Layer." Viewgraphs of the presentation are published in Electromagnetics Laboratory Report 85-1 under the same title.

2. C. S. Lee, S. W. Lee, and S. L. Chuang, "Plot of Modal Field Distribution in Rectangular and Circular Waveguides," IEEE Trans. Microwave Theory and Tech., Vol. MTT-33, pp. 271-274, March 1985.

3. C. S. Lee, S. L. Chuang, and S. W. Lee, "A Simple Version of Corrugated Waveguide: Smooth-Walled Circular Waveguide Coated with Lossy Magnetic Material," to be presented at 1985 International IEEE/AP-S Symposium, Vancouver, B.C., Canada, June 1985; also to be presented at Seventh Annual Electromagnetics, Propagation and Communication Affiliates Workshop, Urbana, IL, April 1985.

4. C. S. Lee, S. W. Lee, and S. L. Chuang, "Normal Modes in an Overmoded Waveguide Coated with Lossy Material," in preparation, to be submitted for publication in IEEE Trans. Microwave Theory and Tech.

IV. TECHNICAL PROGRESS

Abstract

Major items accomplished in this reporting period are:

1. The dispersions and attenuations of the normal modes in a circular waveguide coated with lossy material are completely analyzed. A magnetic material is recommended for coating. The magnetic material should be less lossy for the high-frequency operation than for the low-frequency operation.

2. The radar cross section (RCS) from a circular waveguide coated with lossy material has been calculated. We have made the following observations:

   (i) The interior irradiation contributes to the RCS much more than does the rim diffraction.

   (ii) At low frequency ($a/\lambda \approx 1$), the RCS from the circular waveguide terminated by a perfect electric conductor (PEC) can be reduced more

than 13 dB down with a coating thickness less than 1% of the radius using the best lossy material available in a 6 radius-long cylinder.

(iii) At high frequency ($a/\lambda > 10$), a modal separation between the highly attenuated and the lowly attenuated modes is evident if the coating material is too lossy. With a less lossy material, the RCS reduction over a wide range of the incident angle may be difficult, unless the coating layer is very thick.

However, a large RCS reduction can be achieved for a small incident angle with a thin layer of coating.

3. As a by-product of this research, we have found that the waveguide coated with a lossy magnetic material can be used as a substitute for a corrugated waveguide to produce a circularly polarized radiation field.

Details are explained below.

(1) Analysis of the normal modes in a waveguide coated with lossy material

At low frequency, as indicated earlier [1], a magnetic material has been suggested over a dielectric material for coating. The physical reason for this is the following. The attenuation constant of a normal mode is proportional to the power dissipation which, in turn, is directly related to the electric energy of the normal mode within the lossy dielectric layer or to the magnetic energy within the lossy magnetic layer. The magnetic field is large near the surface when the perturbation of the field due to the coating is small. Thus, the magnetic coating results in a larger attenuation constant for the normal mode than the dielectric coating. This idea has been already investigated experimentally for the application of an attenuator [2], [3].

At high frequency, the modal-field distribution in the coated waveguide is much different from that in the uncoated waveguide and the argument based on the quasi-static approximation breaks down [1]. Figure 1 shows the attenuation

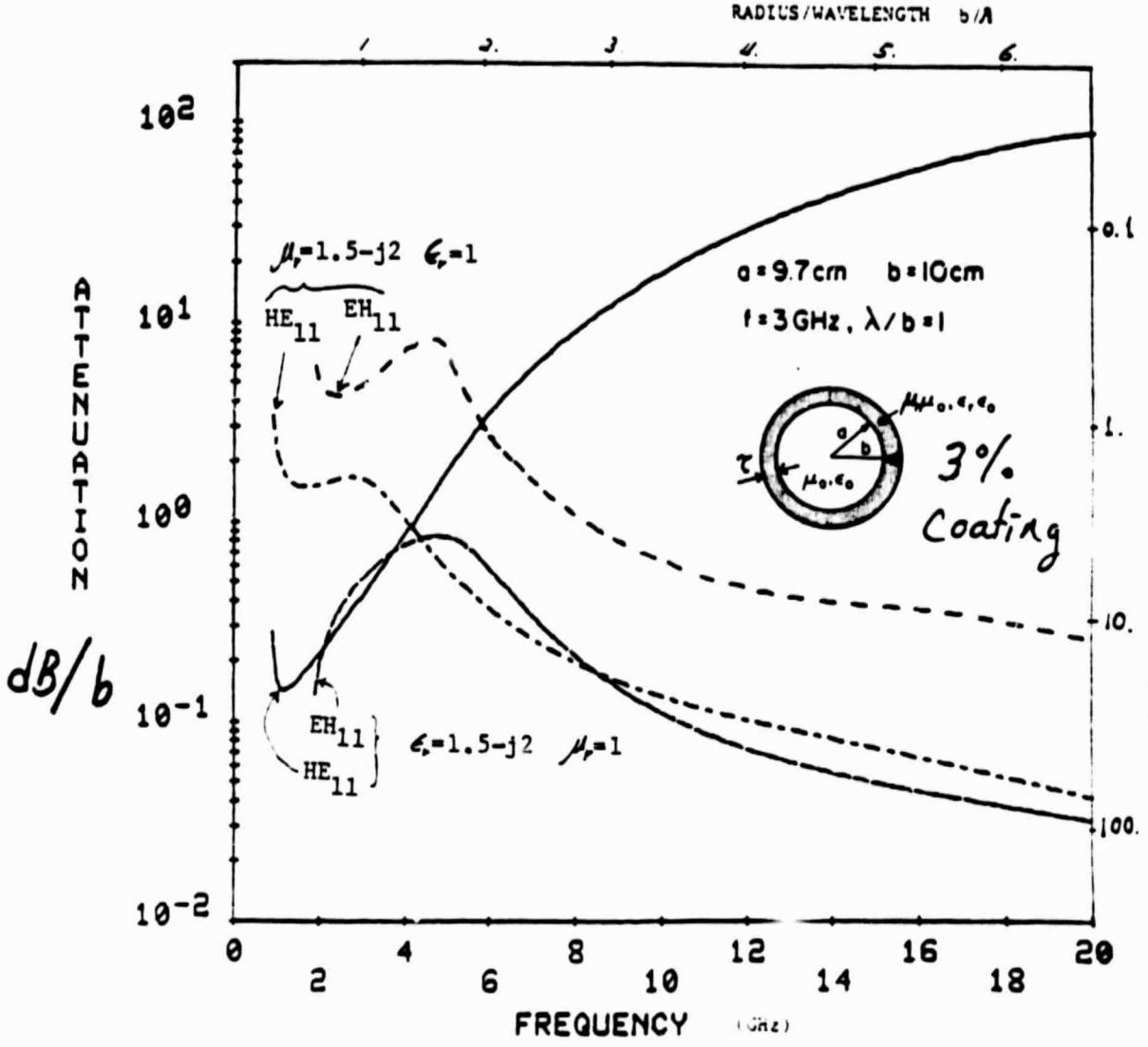

Figure 1. Attenuation constants as a function of frequency for both magnetic ($\epsilon_r = 1$, $\mu_r = 1.5 - j2$) and dielectric coatings ($\mu_r = 1$, $\epsilon_r = 1.5 - j2$).

properties of the normal modes in a waveguide coated with a magnetic material and a dielectric material. The dielectric constant of the dielectric material is set equal to the relative permeability of the magnetic material for the purpose of comparison. At the low frequency ($a/\lambda \sim 1$), the magnetic coating results in the large attenuation constants for the normal modes. However, at the high frequency ($a/\lambda \gtrsim 3$), the attenuation behavior of the normal modes is quite different from that at the low frequency. This is the area we have investigated further for the past six months.

In the past, the properties of the normal modes in an overmoded waveguide were investigated for the low-loss [4], [5], [6] and the high-loss cases [7]. The case between these two extremes is of interest to us, but it appears that this case needs to be further investigated.

When the coating material is lossless, all the normal modes become surface waves (or slow waves) as the layer thickness increases, in the order of HE_{n1}, EH_{n1}, HE_{n2}, EH_{n2}, where $n \neq 1$ and EH_{01}, HE_{01}, EH_{02}, HE_{02}, ... [5]. This behavior of the normal modes is shown in Figure 2 for a dielectric coating and in Figure 3 for a magnetic coating, where the radial wave numbers, $k_{\rho l}$'s, are plotted as a function of the layer thickness. The large imaginary part of the radial wave number indicates that the modal field shifts to the wall, i.e., the mode becomes a surface wave. Note that the onset of a new surface wave occurs around every quarter-wavelength thickness.

When the loss tangent of the coating material is small, the general trend of the normal modes remains similar to that for the waveguide coated with a lossless material (Figures 4 and 5). As shown in Figures 6 and 7, the surface mode (i.e., the mode with a large imaginary part of the radial wave number) has a large attenuation constant. One interesting fact to be noted is

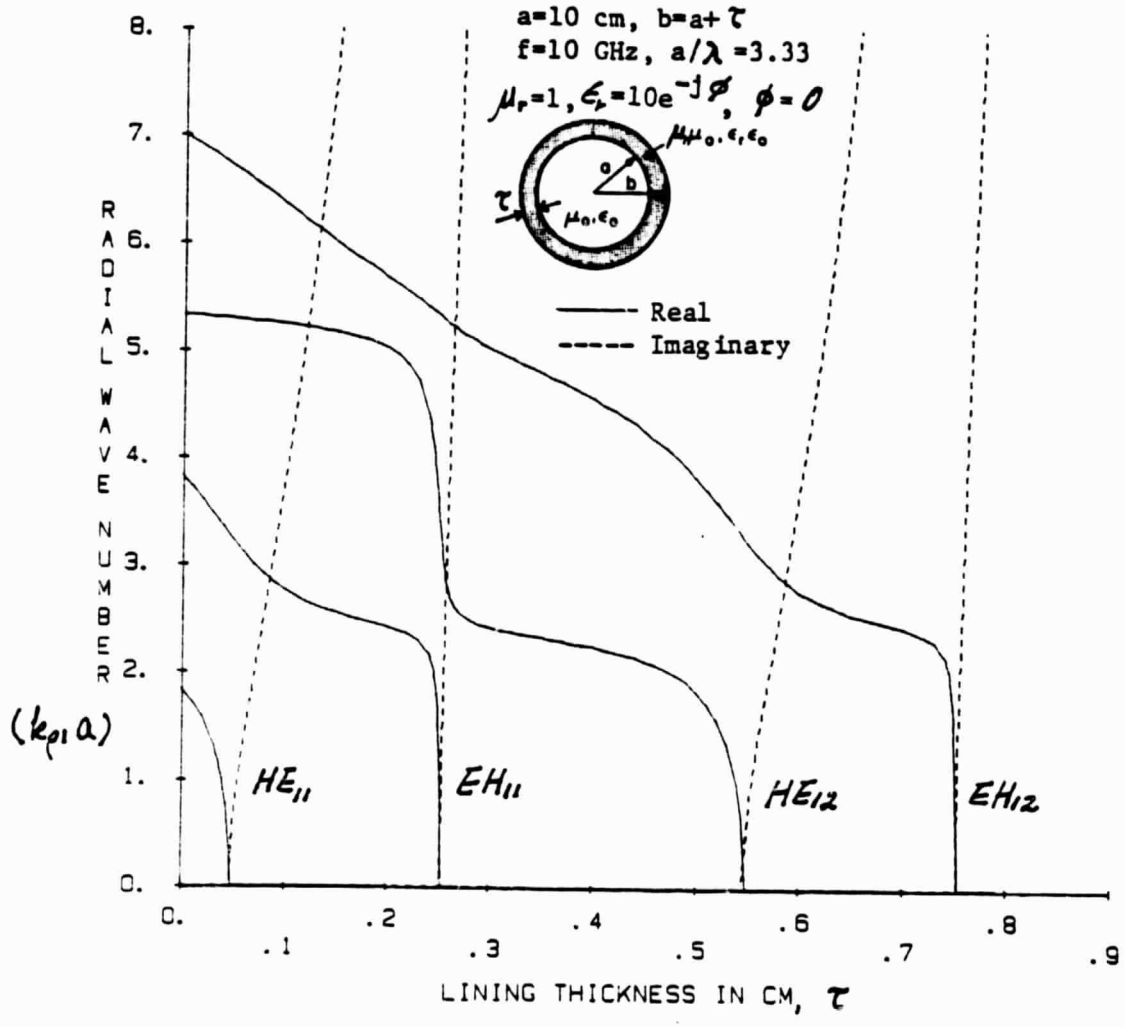

Figure 2. Radial wave numbers of the normal modes in a waveguide coated with a lossless dielectric material ($\mu_r = 1$, $\varepsilon_r = 10$).

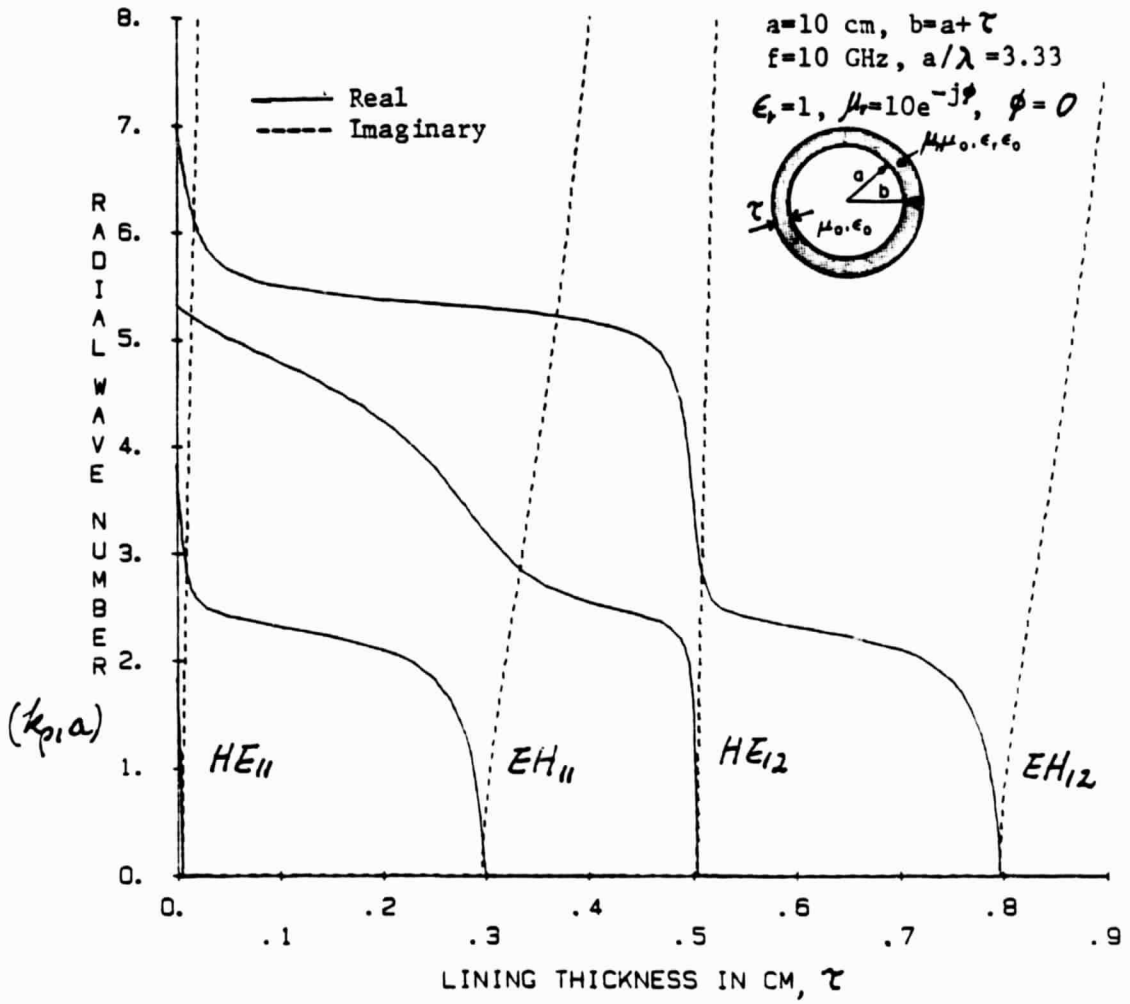

Figure 3. Radial wave numbers of the normal modes in a waveguide coated with a lossless magnetic material ($\varepsilon_r = 1$, $\mu_r = 10$).

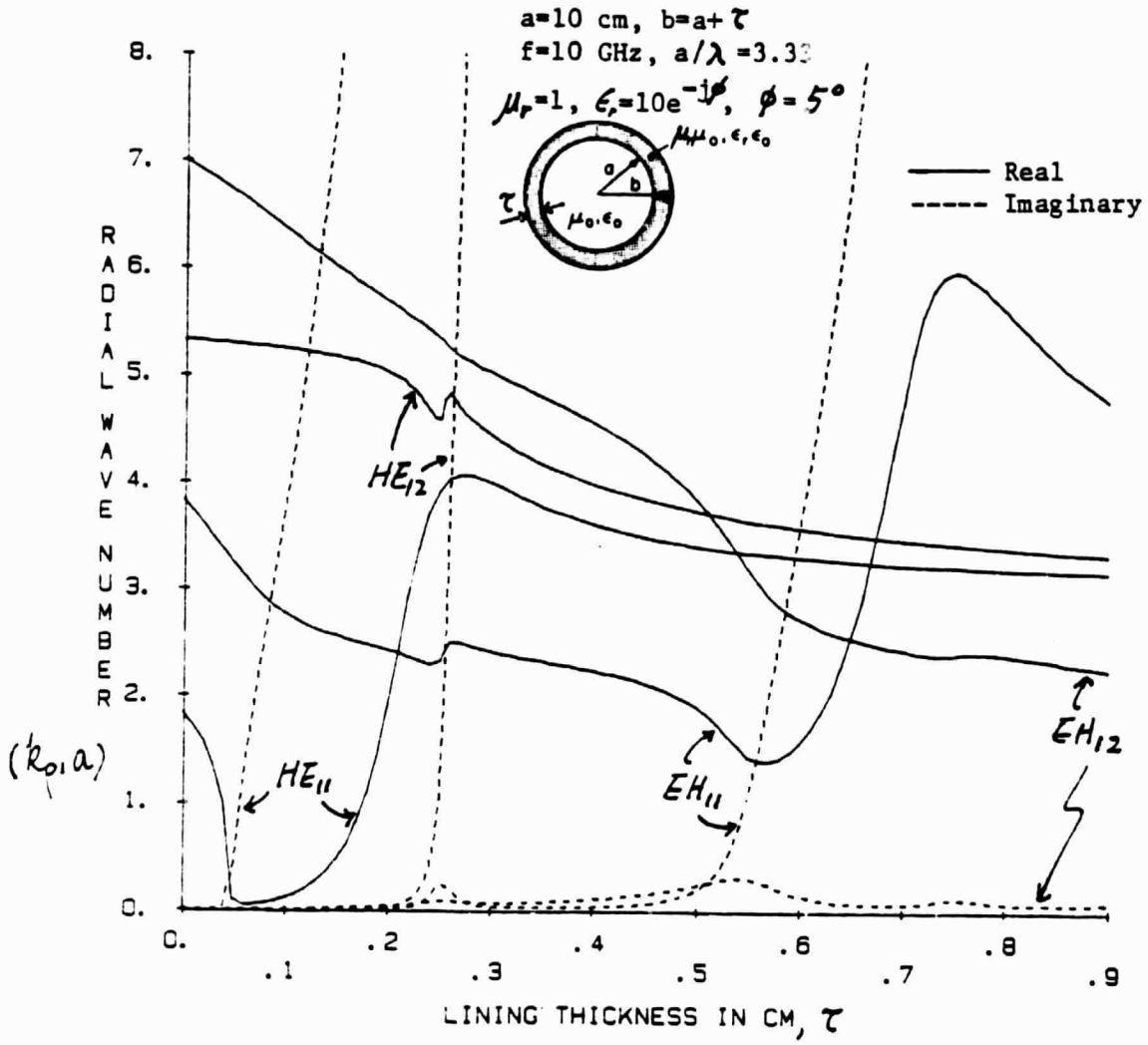

Figure 4. Radial wave numbers of the normal modes in a circular waveguide coated with a lossy dielectric material ($\mu_r = 1$, $\varepsilon_r = 10e^{-j\phi}$, $\phi = 5°$).

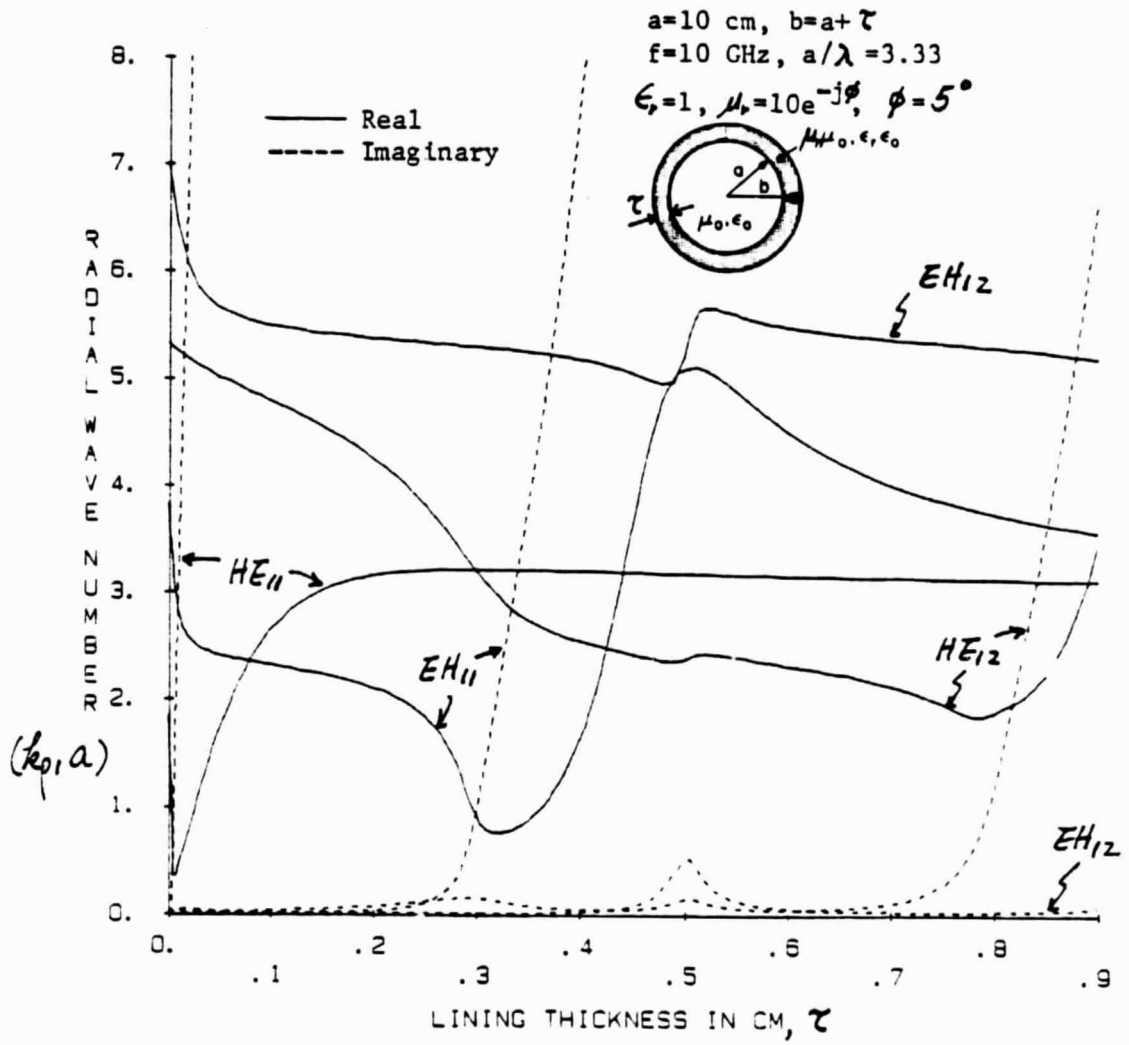

Figure 5. Radial wave numbers of the normal modes in a circular waveguide coated with a lossy magnetic material ($\varepsilon_r = 1$, $\mu_r = 10^{-j\phi}$, $\phi = 5°$).

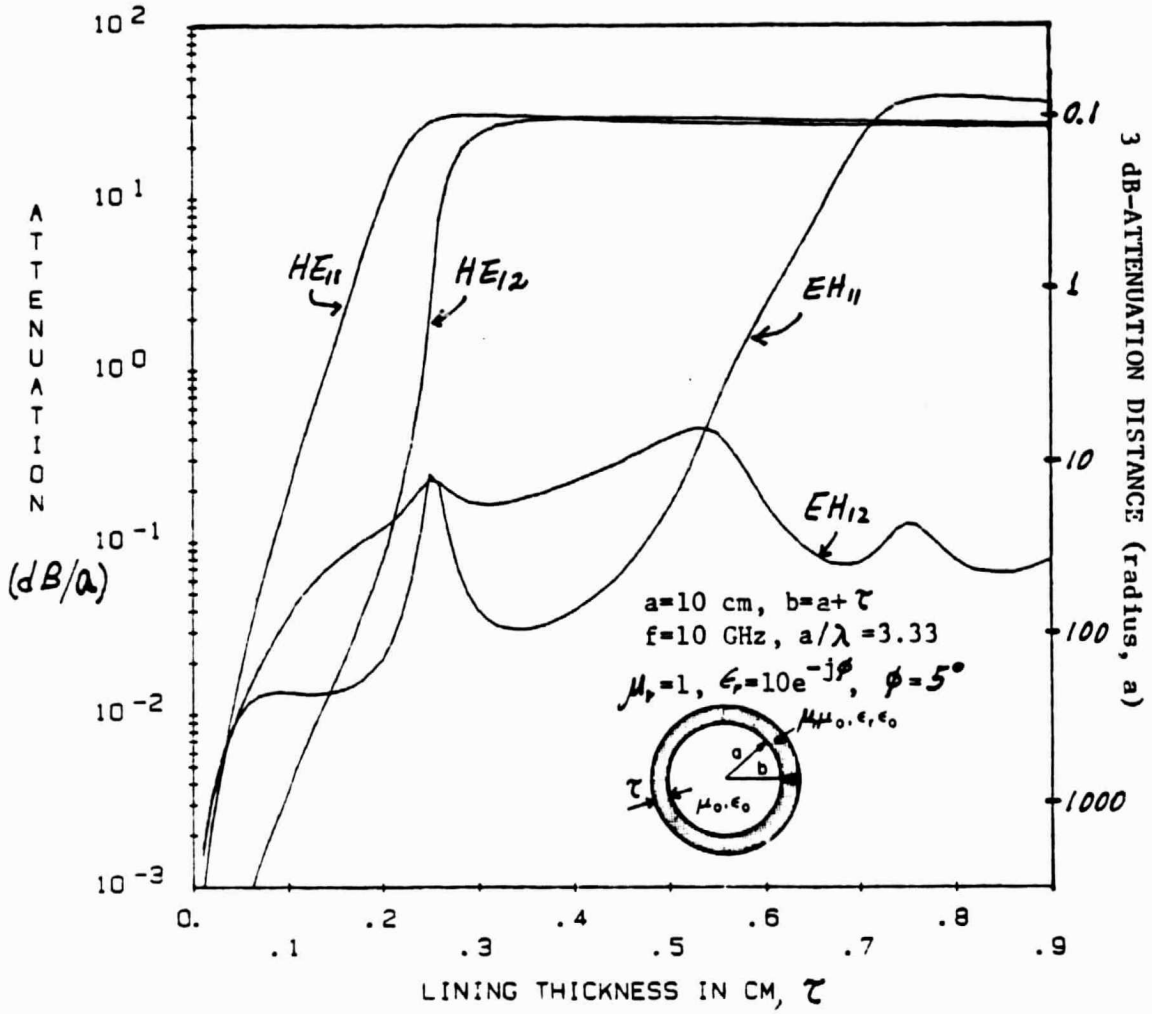

Figure 6. Attenuation constants of the normal modes coated with a lossy dielectric material ($\mu_r = 1$, $\varepsilon_r = 10e^{-j\phi}$, $\phi = 5°$).

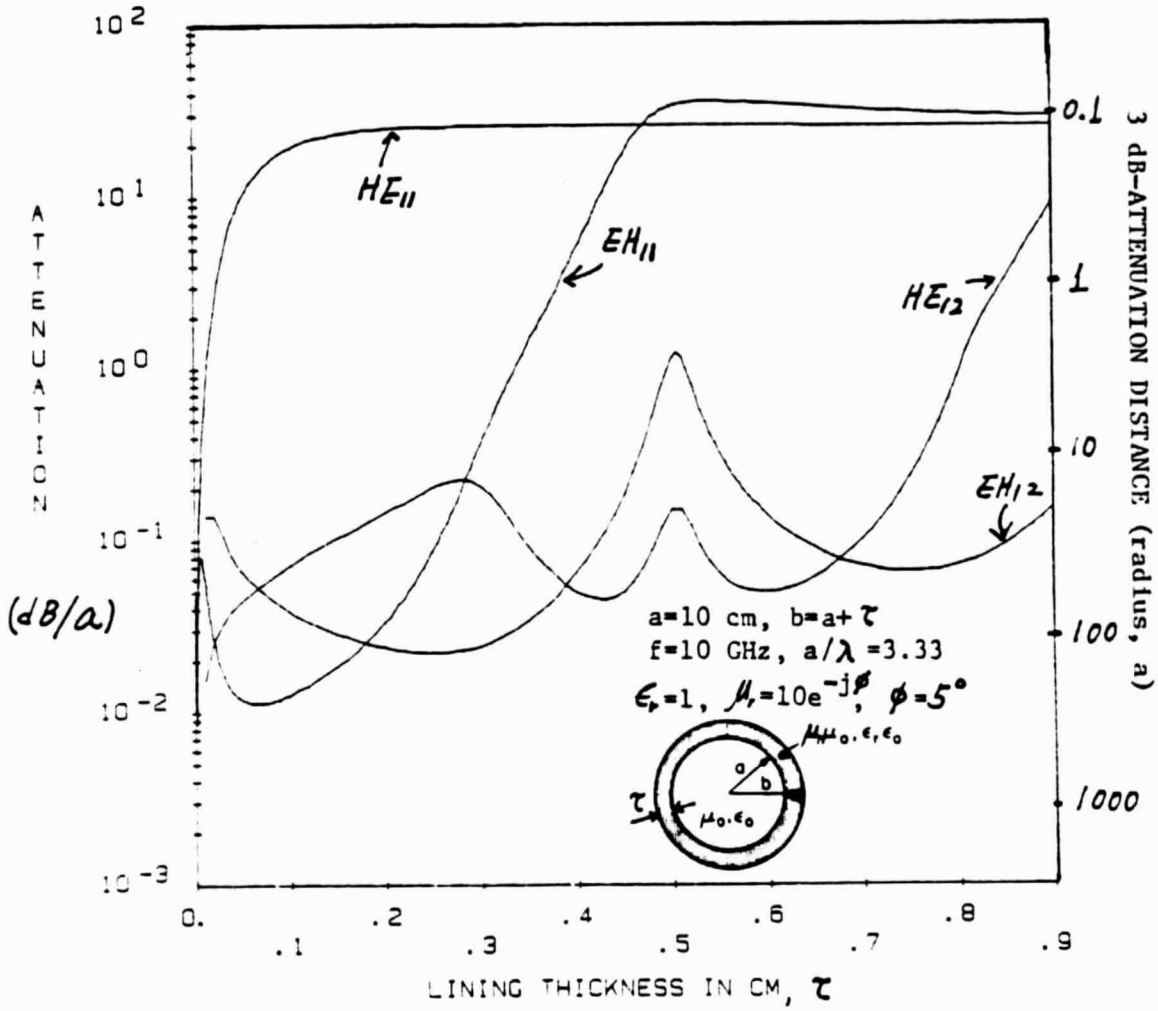

Figure 7. Attenuation constants of the normal modes coated with a lossy magnetic material ($\varepsilon_r = 1$, $\mu_r = e^{-j\phi}$, $\phi = 5°$).

that in the dielectric coating the order of the EH_{11} and HE_{12} modes becoming the surface modes as the lossy-layer thickness increases is reversed from that in the waveguide coated with a lossless material. This indicates that the dielectric coating attracts the HE_{12} mode more than the EH_{11} mode. This is a hint of a modal separation between the highly attenuated modes of a surface-mode type and the lowly attenuated modes of an inner-mode type. This feature is clearly evident when the material is very lossy as shown in Figures 8, 9, 10 and 11 ($\phi = 45°$). The summary of the modal separation is shown in Table 1. Note that the roles of the normal modes in a dielectric coating are just opposite to those in a magnetic coating, and the case with the angular index, $m \neq 0$, is different from all other cases with $m \neq 0$.

From the above results, we draw the following important conclusions for the high-frequency case:

(i) When the loss tangent of the coating material is sufficiently small, eventually every mode becomes the surface-type mode as the layer thickness increases. If the coating material is lossy enough, these surface-type normal modes will have large attenuation constants. When these two conditions are satisfied, then all the modes in the waveguide can be attenuated significantly in a short traveling distance if the lossy layer is thick enough. In a practical application, we need to find a common ground which satisfies both of these two conditions. Unfortunately, at a higher frequency, there is a narrower regime that these conditions are satisfied. When the material is not lossy enough, the mode would not be attenuated much even if it became similar to a surface-type mode. When the material is too lossy, there occurs a modal separation between the highly attenuated modes and the

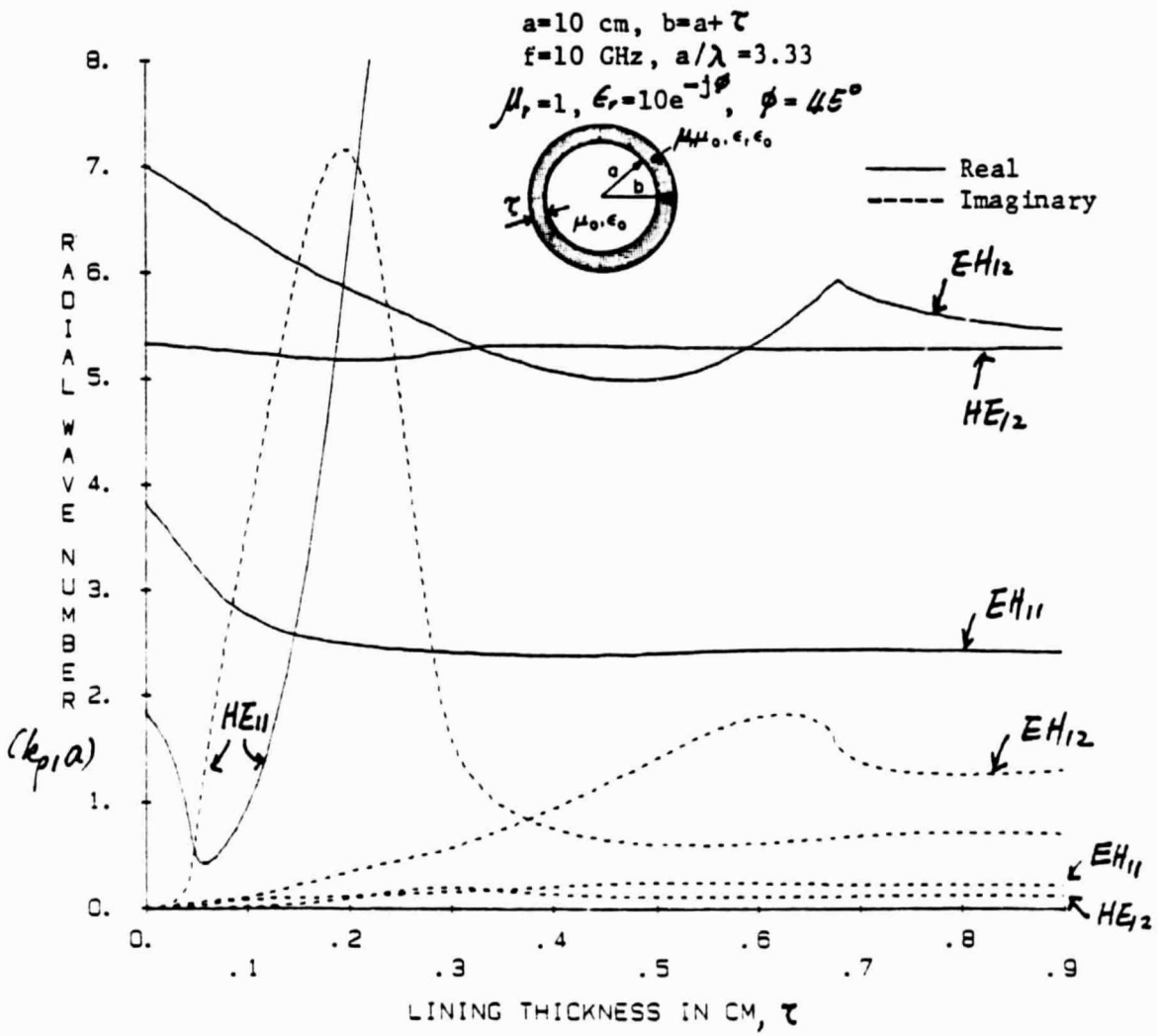

Figure 8. Radial wave numbers of the normal modes in a waveguide coated with a lossy dielectric material ($\mu_r = 1$, $\varepsilon_r = 10e^{-j\phi}$, $\phi = 45°$).

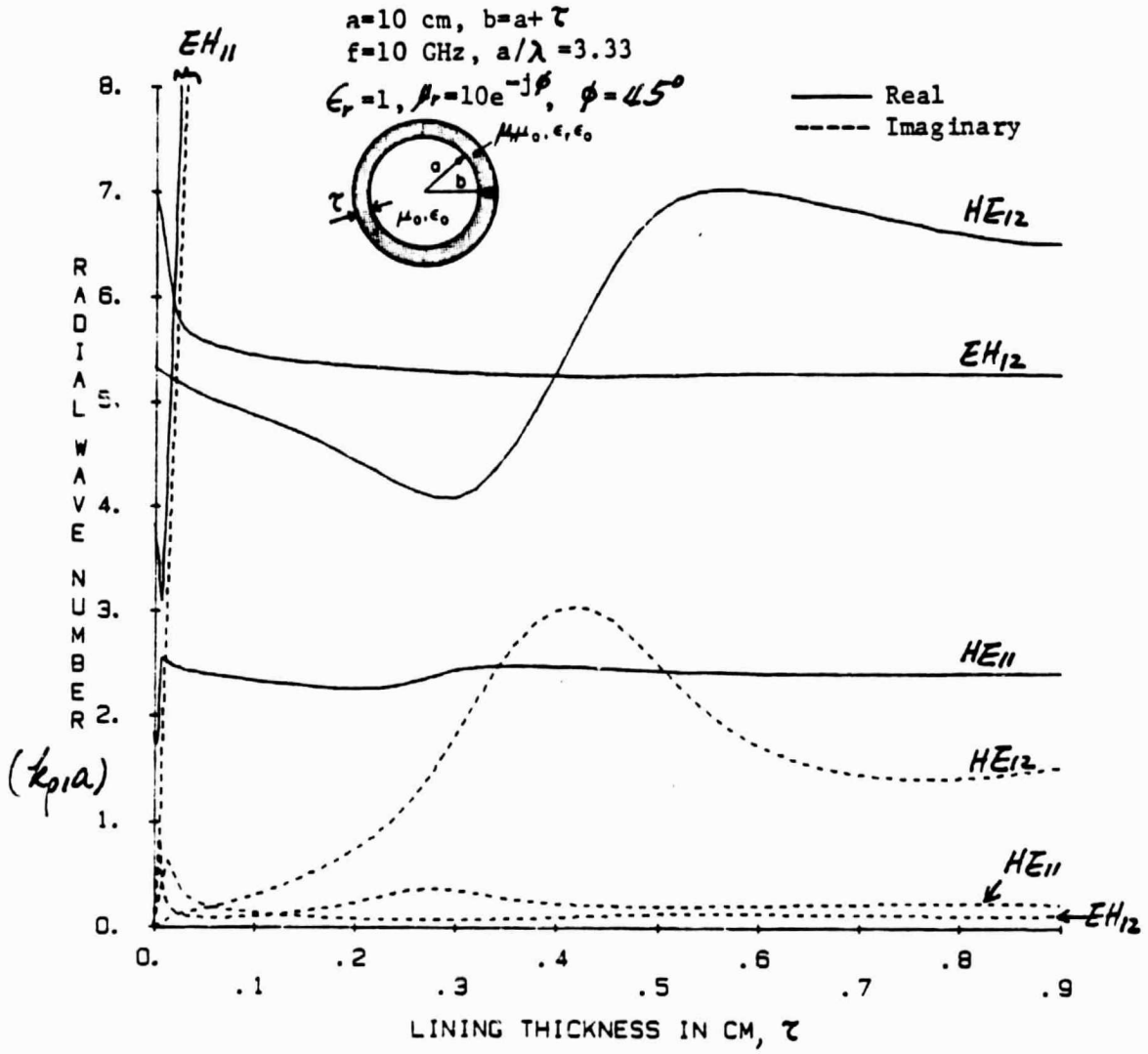

Figure 9. Radial wave numbers of the normal modes in a waveguide coated with a lossy magnetic material (ϵ_r = 1, μ_r = 10e$^{-j\phi}$, ϕ = 45°).

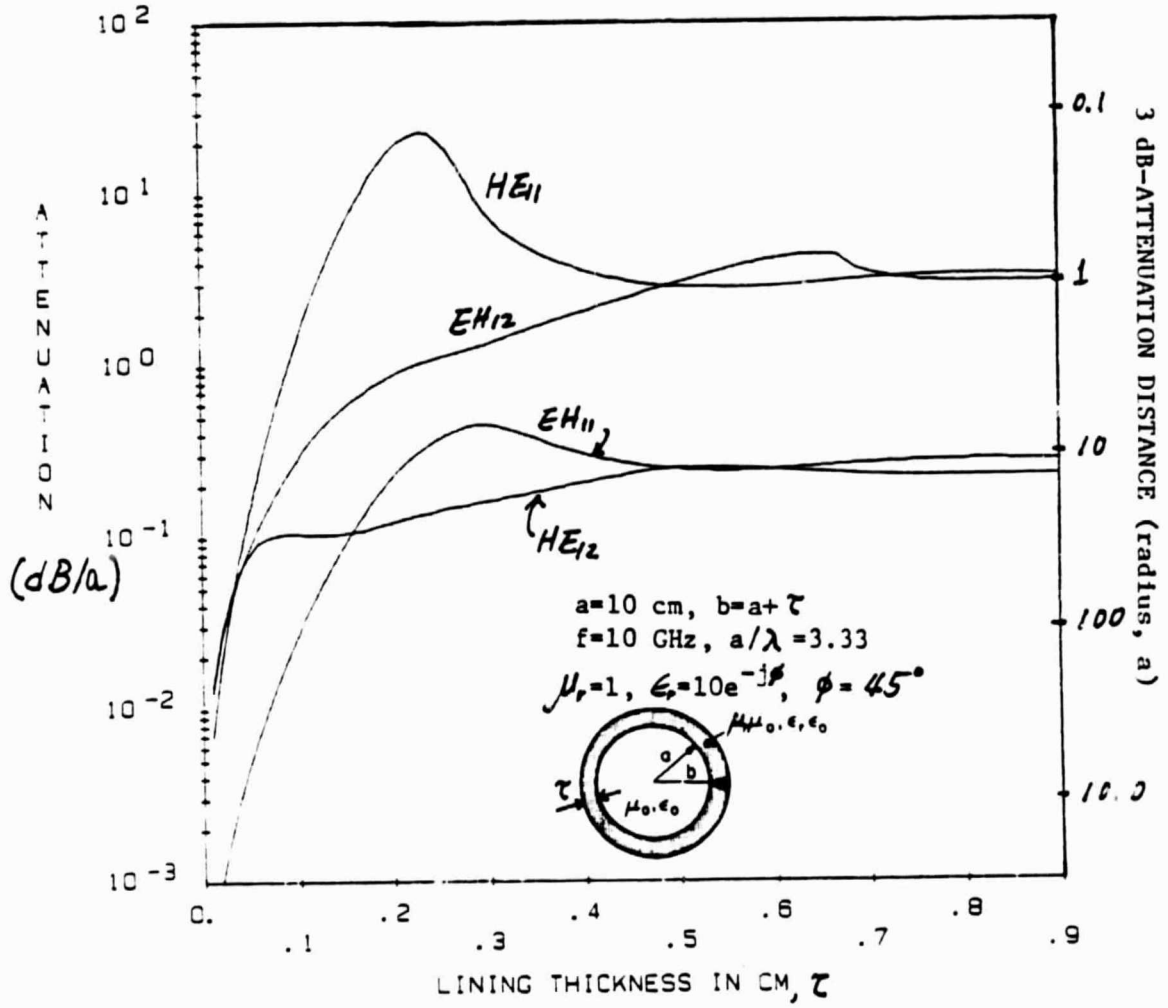

Figure 10. Attenuation constants of the normal modes in a waveguide coated with a lossy dielectric material ($\mu_r = 1$, $\varepsilon_r = 10e^{-j\phi}$, $\phi = 45°$).

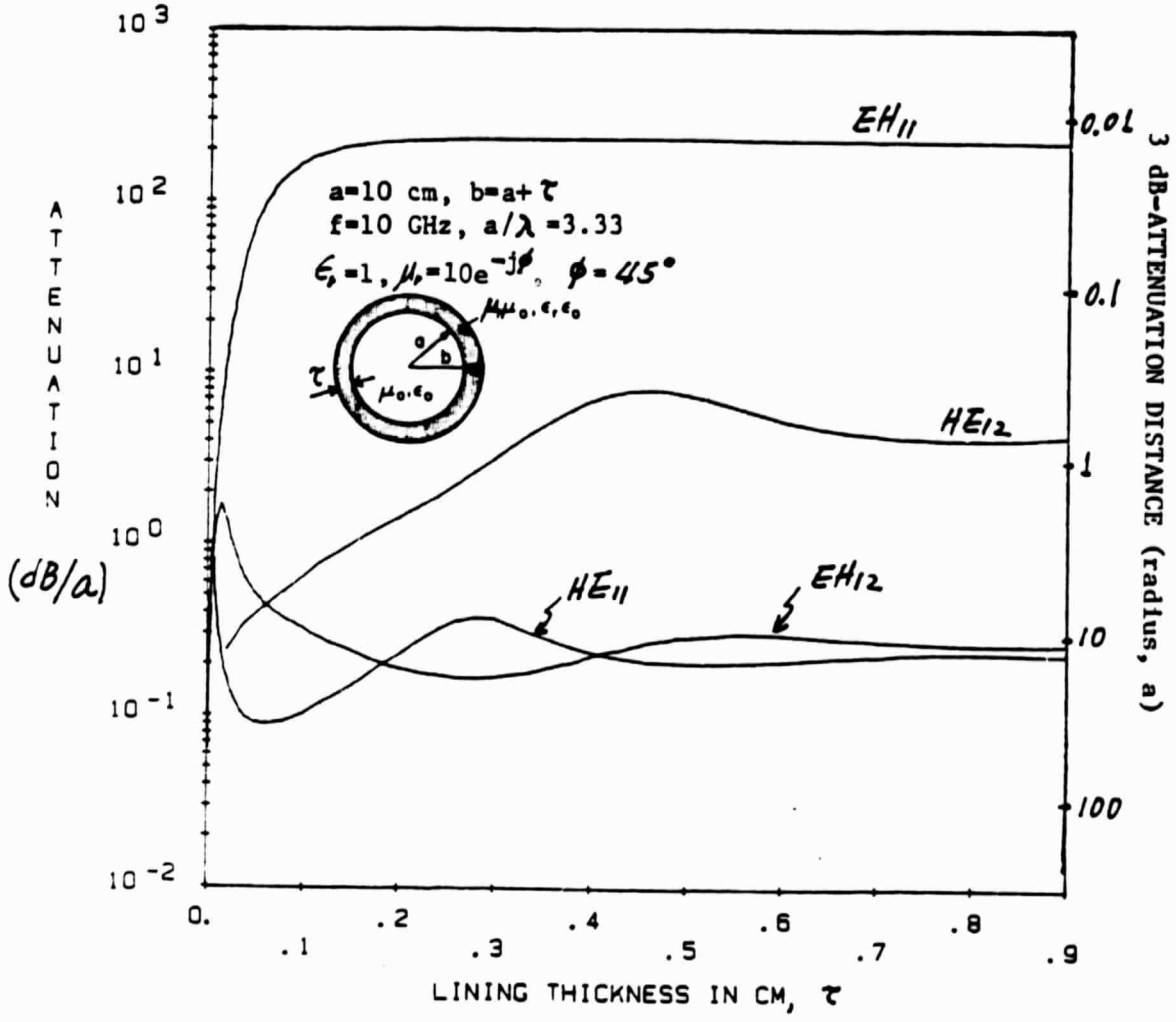

Figure 11. Attenuation constants of the normal modes in a waveguide coated with a lossy magnetic material ($\varepsilon_r = 1$, $\mu_r = 10e^{-j\phi}$, $\phi = 45°$).

TABLE 1.

MODAL SEPARATION IN AN OVERMODED WAVEGUIDE COATED WITH A LOSSY MATERIAL

Dielectric Coating	
High Attenuation	Low Attenuation
EH_{01}, HE_{on}, $n=2,3,\ldots$; HE_{m1}, EH_{mn} $\left.\begin{matrix} m=1,2,\ldots \\ n=2,3,\ldots \end{matrix}\right\}$	HE_{01}, EH_{on}, $n=2,3,\ldots$; EH_{m1}, HE_{mn} $\left.\begin{matrix} m=1,2,\ldots \\ n=2,3,\ldots \end{matrix}\right\}$
Low Attenuation	High Attenuation
Magnetic Coating	

lowly attenuated modes (Table 1). This is not desirable for the RCS reduction from the waveguide because the unattenuated modes will cause a large RCS at a certain incident angle.

(ii) As will be shown in Section 2 of this report, the lower-order modes are mostly responsible for the RCS from a waveguide by an incident plane wave with a small incident angle. Thus in reducing the RCS for a small incident angle, the layer-thickness can be very small even if the modal separation may occur.

(iii) As will be explained in Section 2, the coating must be gradual from the mouth to the inner side of the cylinder so that the transition from the modes at the mouth to those in the inner side of the cylinder becomes smooth. The variation of the modal fields with the layer thickness in the waveguide with a magnetic coating appears to be less drastic than that with a dielectric coating. This may be due to the nature of the boundary conditions of the metallic surface. Thus, the magnetic coating is recommended over the dielectric coating as in the case at the low frequency if all other criteria are the same for both cases.

Finally, we compared our results with the asymptotic calculation by Marcatili and Schmetzer as a/λ becomes very large [7]. The attenuation constants of the lowly attenuated modes of the inner mode type in our calculation agree well with their results, but those of the highly attenuated modes of the surface-mode type become close to their results at a much larger value of a/λ than that for the case of the lowly attenuated modes.

While we were investigating the properties of the normal modes, we found that the HE_{11} mode in a waveguide coated with a very lossy magnetic material shows an interesting property which can be useful in a practical application. The detailed picture of Figure 9 for a very thin layer is shown in Figure 12. Usually, the HE_{11} mode becomes a surface wave in a waveguide with a thin coated layer (Figures 4, 5, and 8). However, when the coating magnetic material is very lossy, it becomes an inner mode, which can be used as a substitute for a corrugated waveguide (Figure 12). See Section 3 of this report for details. Note that as the layer thickness increases, the propagation constants of the HE_{11} and EM_{11} modes become nearly equal before the HE_{11} mode becomes an inner mode and the EM_{11} mode becomes a surface mode. When the loss tangent of the magnetic material is larger, the separation between these modes is greater (Figure 13). There may be an "accidental" degeneracy between the HE_{11} and EH_{11} modes in a waveguide coated with a magnetic material with the magnetic loss tangents between 5° (Figure 5) and 45° (Figure 12).

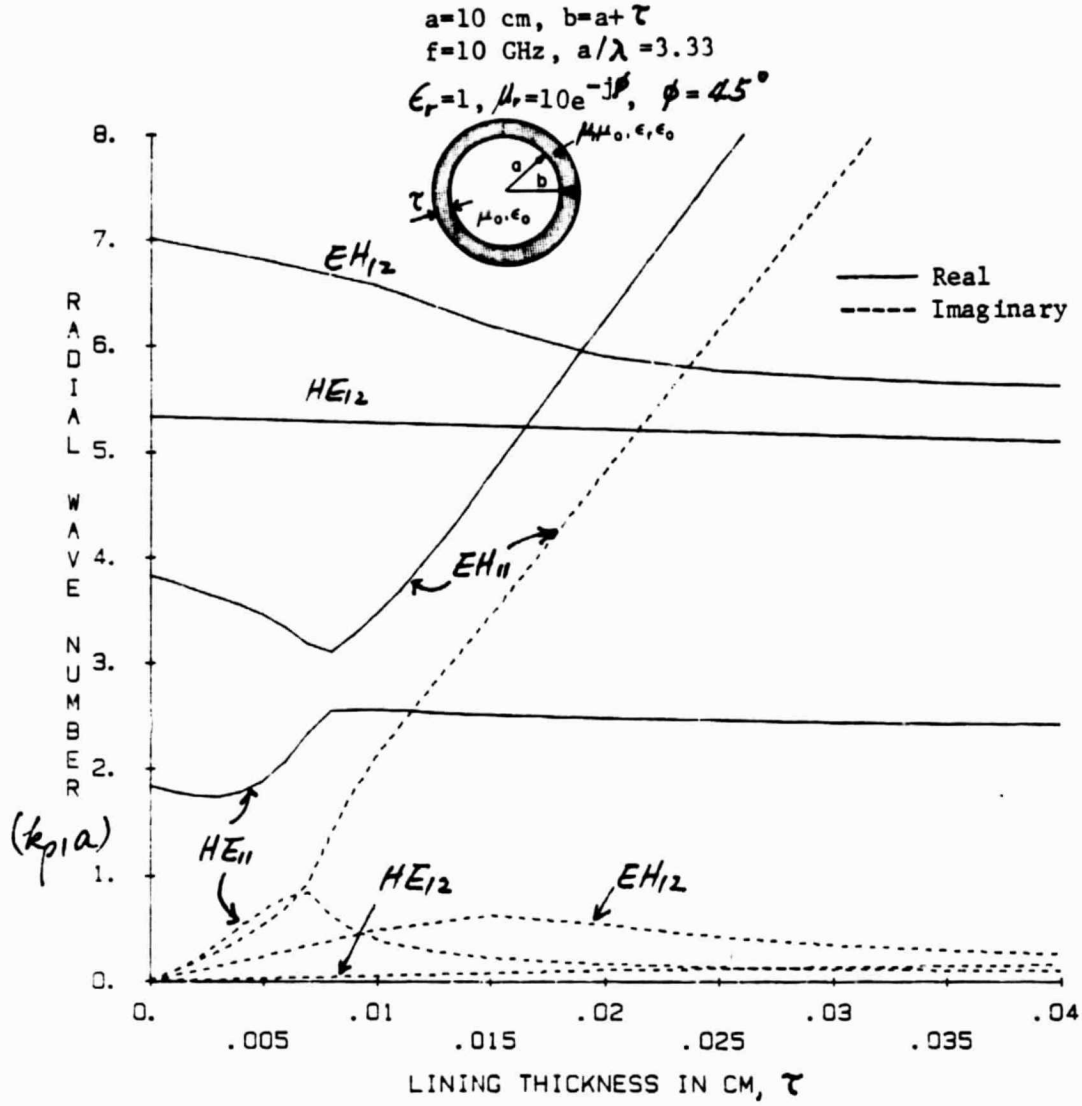

Figure 12. Radial wave numbers of the normal modes in a waveguide coated with a lossy magnetic material (expanded version of Figure 9) (ε_r = 1, μ_r = 10e$^{-j\phi}$, ϕ = 45°).

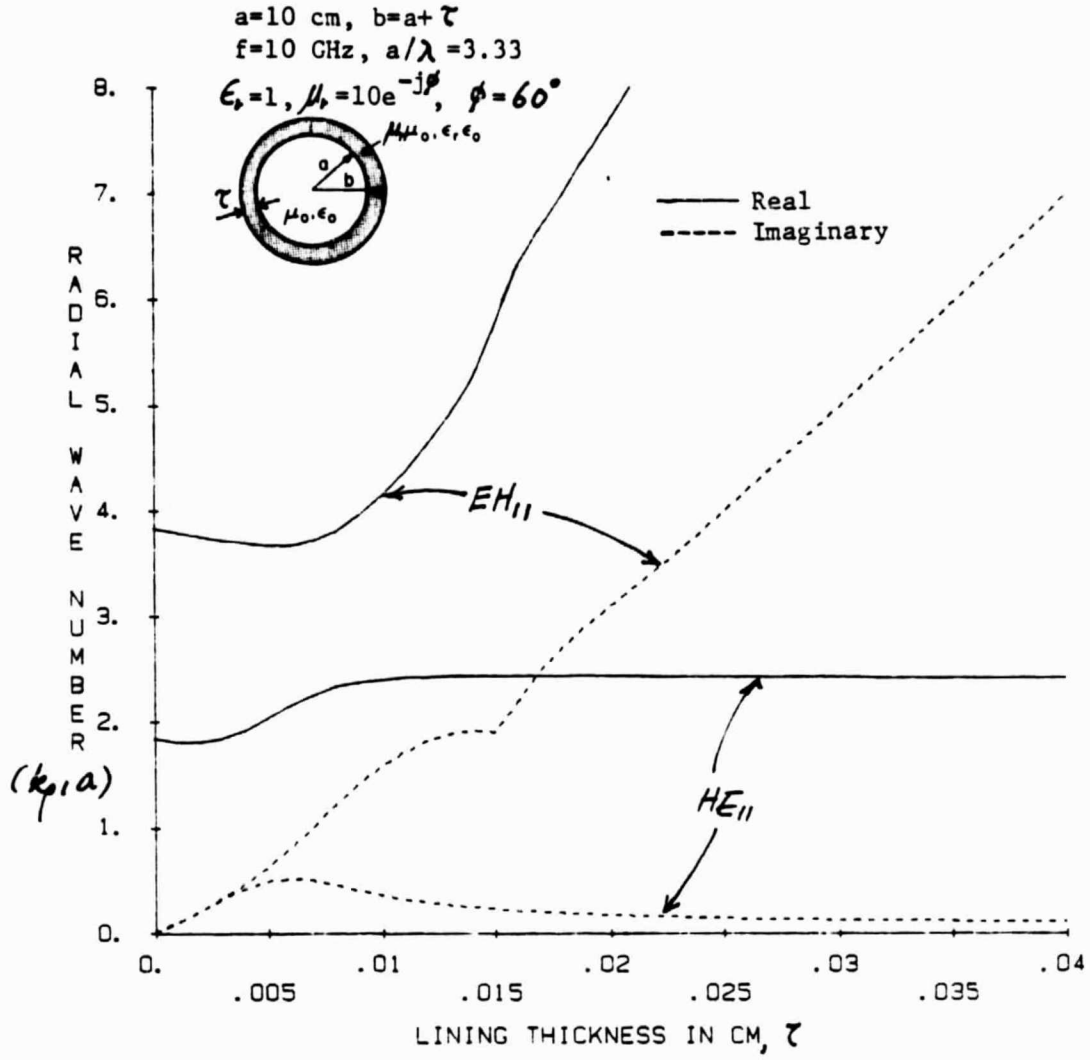

Figure 13. Radial wave numbers of the normal modes in a waveguide coated with a lossy magnetic material (ε_r = 1, μ_r = 10e$^{-j\phi}$, ϕ = 60°).

(2) The RCS calculation

There are three steps in calculating the radar cross section (RCS) from the lossy waveguide (Figure 14):

(i) Find the excited normal modes at the waveguide opening due to the incident plane wave.

(ii) Calculate the propagation constants of those transmitted normal modes and find the field distribution at the waveguide after the normal modes are reflected from the PEC termination and reach the opening.

(iii) Evaluate the radiated energy in the direction of the incident plane wave from the field distribution at the opening in step (ii) above.

For step (ii), the propagation constants of the normal modes have been discussed in Section 1 in this report. At the PEC termination, the direction of the wave propagation is reversed with a 180° phase change. We will neglect the effect of the multiple bouncing of the normal modes between the opening and the termination. Since the multiple bouncing reduces the transmitted energy further down before the energy is reemitted, our calculation is more conservative, i.e., this solution indicates the lower bound of the RCS reduction. Since the radius of the cylinder is usually larger than the free-space wavelength, we expect the error due to this assumption would be small [8].

In the Kirchhoff's approximation, the choice between the matchings of the tangential electric field (E matching) and the tangential magnetic field (H matching) at the interface between the two regions is arbitrary [9]. Figure 15 shows the amplitudes of the dominant TE_{11} mode in a cylindrical waveguide excited by a normally incident plane wave using those two Kirchhoff methods

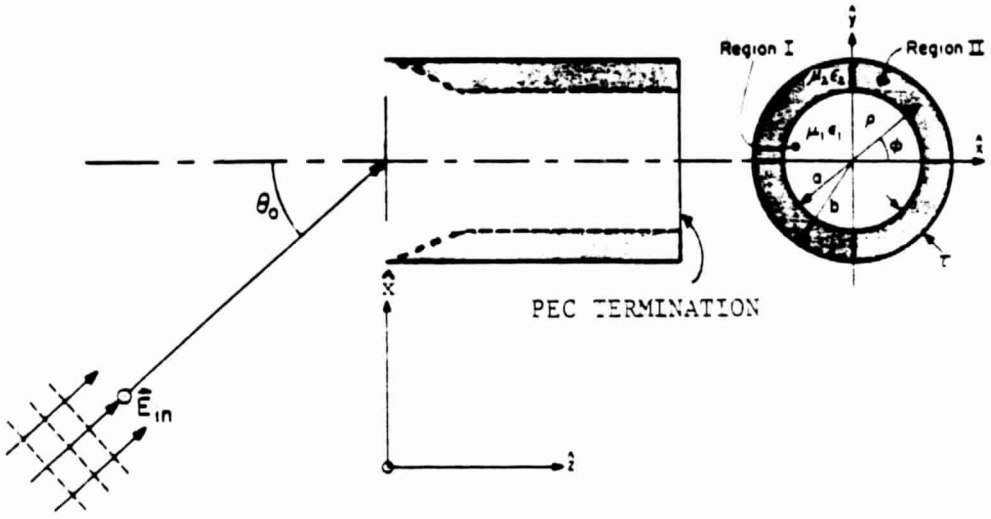

Figure 14. A PEC-terminated cylindrical waveguide coated with a lossy material is illuminated by an incident plane wave.

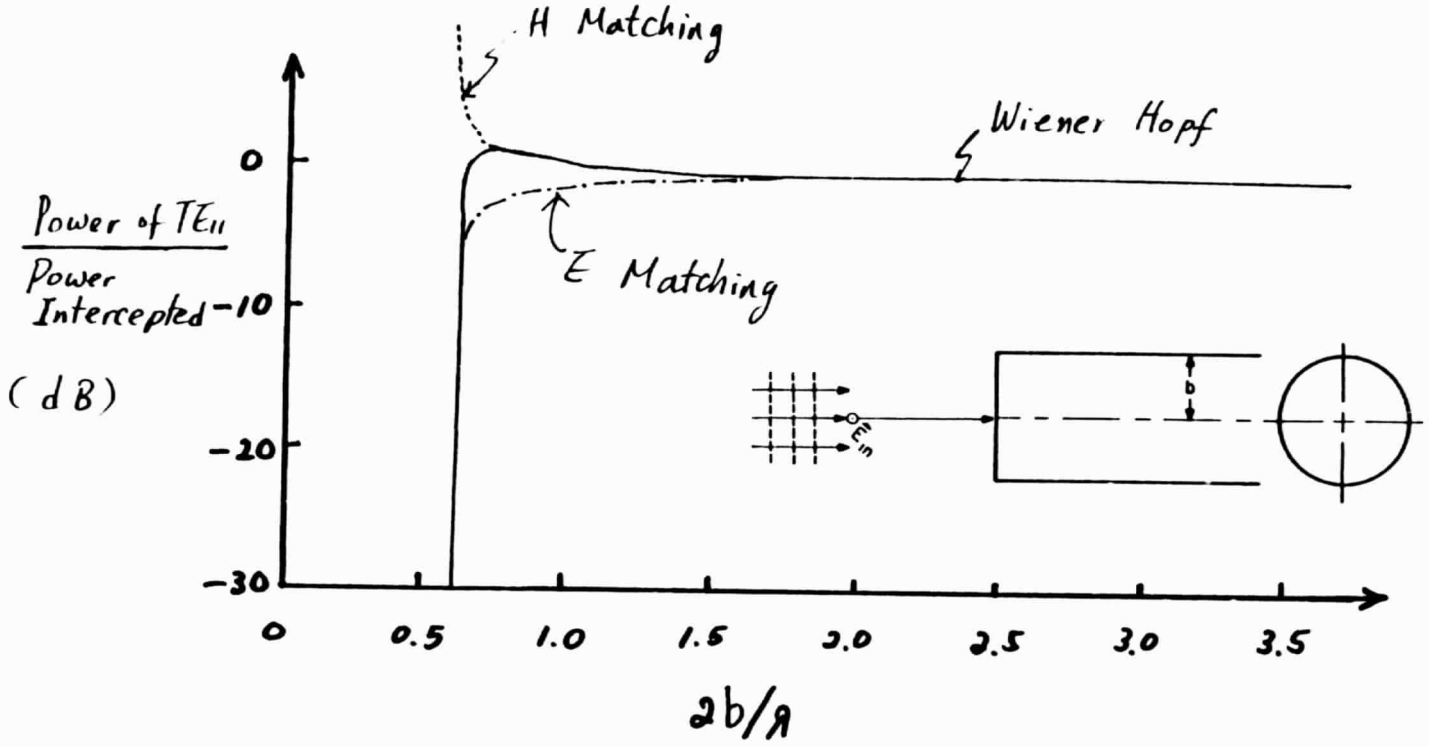

Figure 15. The power of the TE_{11} mode transmitted to a circular waveguide from a normally incident plane wave using the Kirchhoff method and Wiener Hopf technique [10].

and the Wiener Hopf technique which is considered to provide an exact solution [10]. The Kirchhoff approximation is excellent except near the cut-off region. Note that the H matching is better than the E matching except very near the cut-off region. The Kirchhoff approximation assumes that the tangential component of either the electric or magnetic field of the incident field is equal to the sum of all the tangential components of the transmitted normal modes in the waveguide. However, this is an approximation because there is a diffracted field from the edge of the cylinder. In other words, the incident field induces currents on the edge of the cylinder, which reradiate the energy. If the curvature of the rim is not too small, we can see that the reradiated wave has a small tangential component of the magnetic field at the plane of the waveguide opening (Figure 16). For this reason, we choose the matching of the tangential magnetic field assuming that the frequency is not near the cut-off frequency.

Since the propagation constants of the normal modes strongly depend on the frequency, we will divide the problem into three cases which will be considered separately: Low-, intermediate- and high-frequency cases. At the low frequency ($a/\lambda \simeq 1$, a = radius, λ = free space wavelength), the modal-field distribution in the coated waveguide is not much different from that in the uncoated waveguide. On the other hand, at the high frequency ($a/\lambda \simeq 13$), the modal-field distribution changes drastically when the waveguide is coated with a lossy material. At the intermediate frequency ($a/\lambda \simeq 3$), the modal shifts due to the coating are evident but moderate. The range of this classification is shown in Figure 17 and is compared with the approximate dimensions of the jet inlets of three modern military aircrafts. For example, we can see from this chart that the calculation for the intermediate frequency is relevant to that for a jet inlet of a B-1B at 2 GHz, F-15C at 3 GHz or F-5E at 6 GHz.

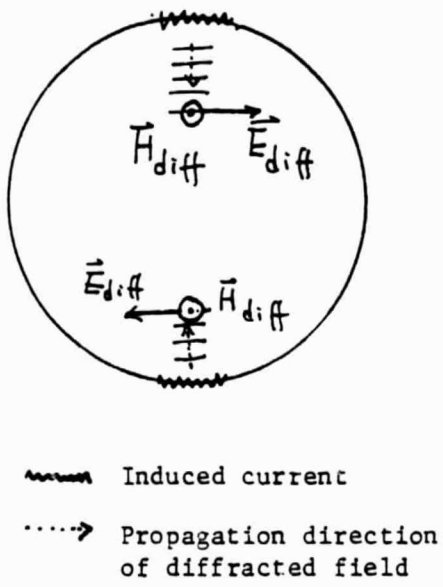

Figure 16. The diffracted field on the plane of the waveguide opening.

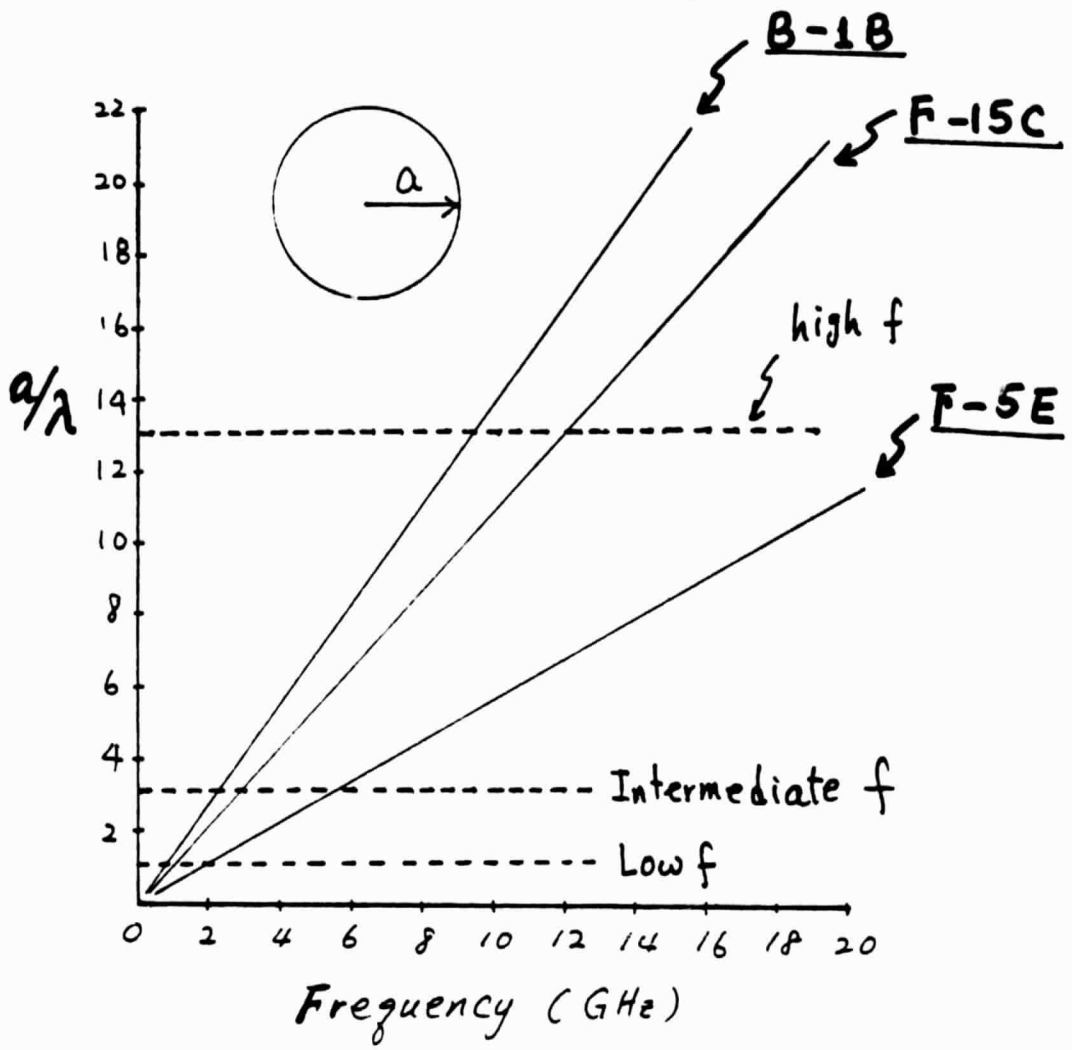

Figure 17. The approximate dimensions of the jet inlets of the three military aircrafts (B-1B, F-15C and F-5E) in terms of the free-space wavelength (Source: Jane's World of Airplane, 83/84).

There are two main sources of the RCS from the cylindrical waveguide: the rim diffraction and the interior irradiation. Figures 18 and 19 show the RCS from these two terms in an uncoated waveguide terminated by a perfect electric conductor (PEC) for $a/\lambda = 1.2$ and 2.3, respectively. Note that the RCS from the interior irradiation is much larger than that from the rim diffraction. Also, we notice that the rim diffraction becomes less important as a/λ increases from 1.2 to 2.3. This can be clearly seen from the results of Johnson and Moffatt [10] as shown in Figure 20. Here the RCS's from the rim diffraction and from the interior irradiation of a ciruclar waveguide for a normal incidence are shown. Johnson and Moffatt assumed that for the interior irradiation all modes except the dominant TE_{11} mode are completely eliminated. In other words, they calculated the RCS due to the excitation of the TE_{11} mode. Clearly, the interior irradiation is far more important than the rim diffraction in computing the RCS except near the cut-off frequencies of the normal modes. Usually the ratio of the RCS to the cross-sectional area of a plate is approximately given by 4π (area/λ^2) [13], and the RCS increases indefinitely with the frequency. In the following calculations, we will neglect the rim diffraction.

Next we compared our solution of the RCS from an uncoated waveguide with other previously reported results as shown in Figure 21. Witt and Price [9] used the Kirchhoff's approximation and included the effect of the multiple bouncing of the normal modes within the waveguide utilizing the transmission-line analogy. Mittra, Lee and Chuang [11] used the Wiener Hopf technique and the generalized scattering matrix to account for the multiple bouncing of the normal modes. These two results agree well with the experimental result by Witt and Price [9]. Our solution is in good agreement with their results when the incident angle is smaller than 45°. Since we are emphasizing the RCS for a small incident angle, our approximation is adequate to serve our purpose.

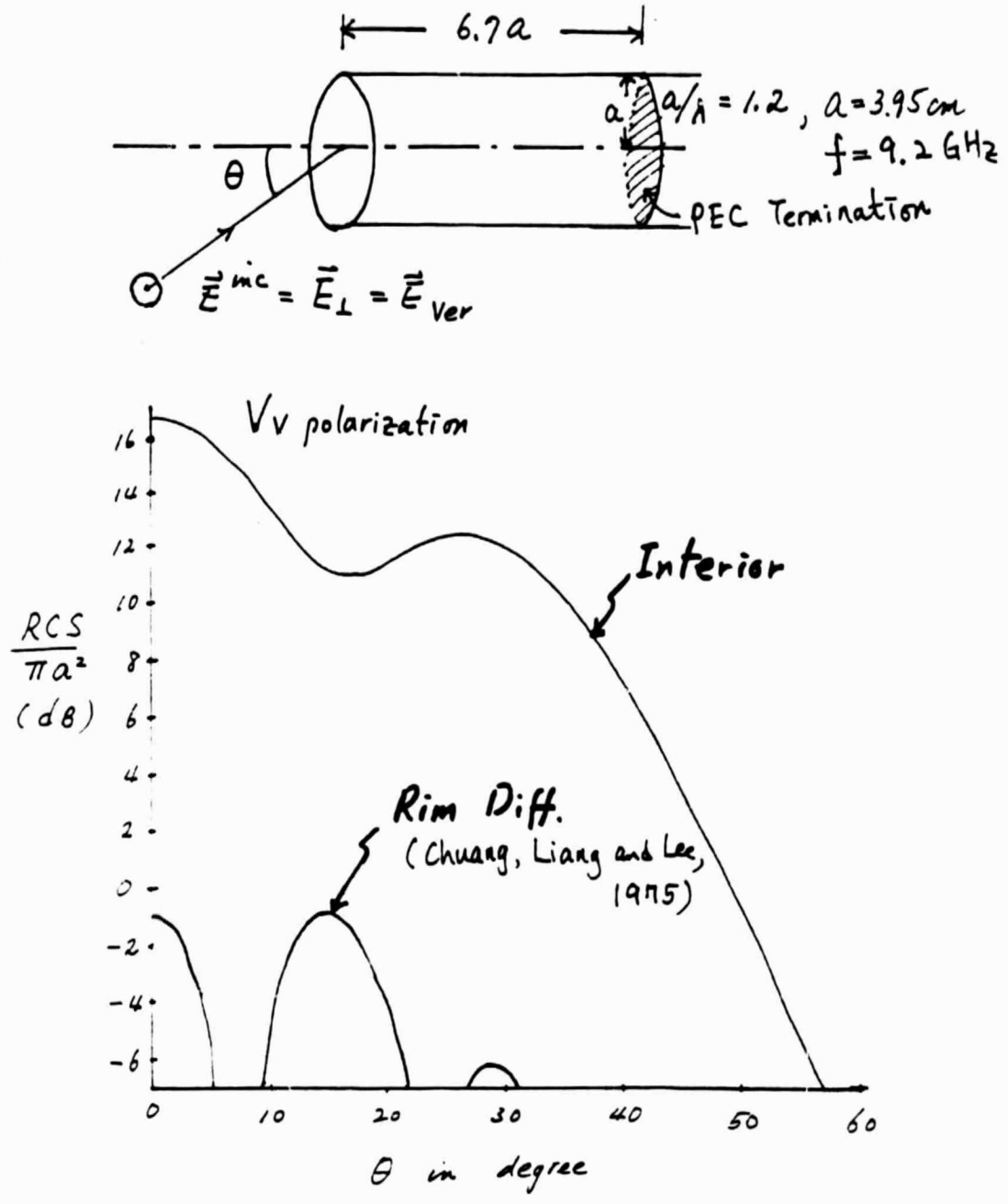

Figure 18. The RCS's from the interior irradiation and the rim diffraction [11] of a circular waveguide terminated by a PEC as a function of the incident angle (a/λ = 1.2, length = 26.46 cm, a = 3.95 cm, vertical polarization).

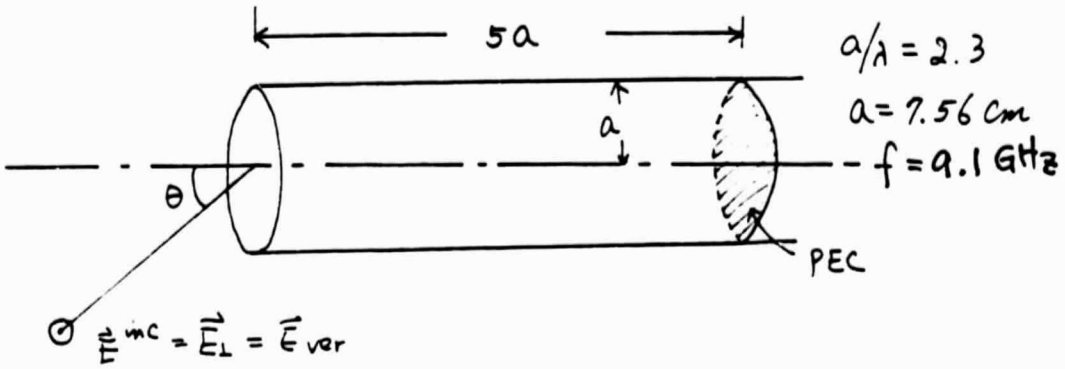

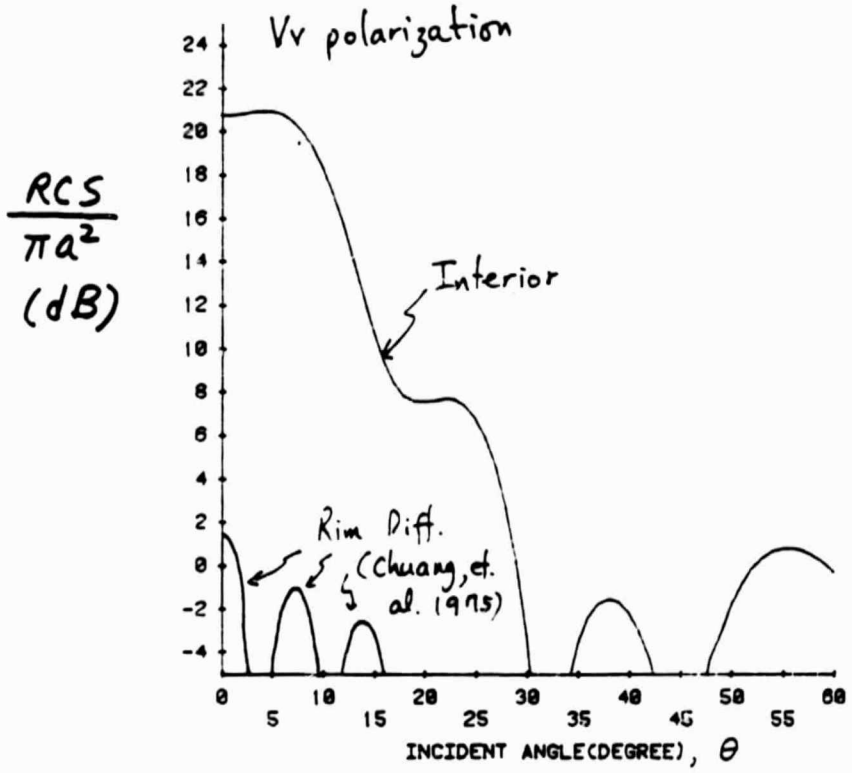

Figure 19. The RCS's from the interior irradiation and the rim diffraction [12] of a circular waveguide terminated by a PEC as a function of the incident angle (a/λ = 2.3, length 37.8 cm, a = 7.56 cm, vertical polarization).

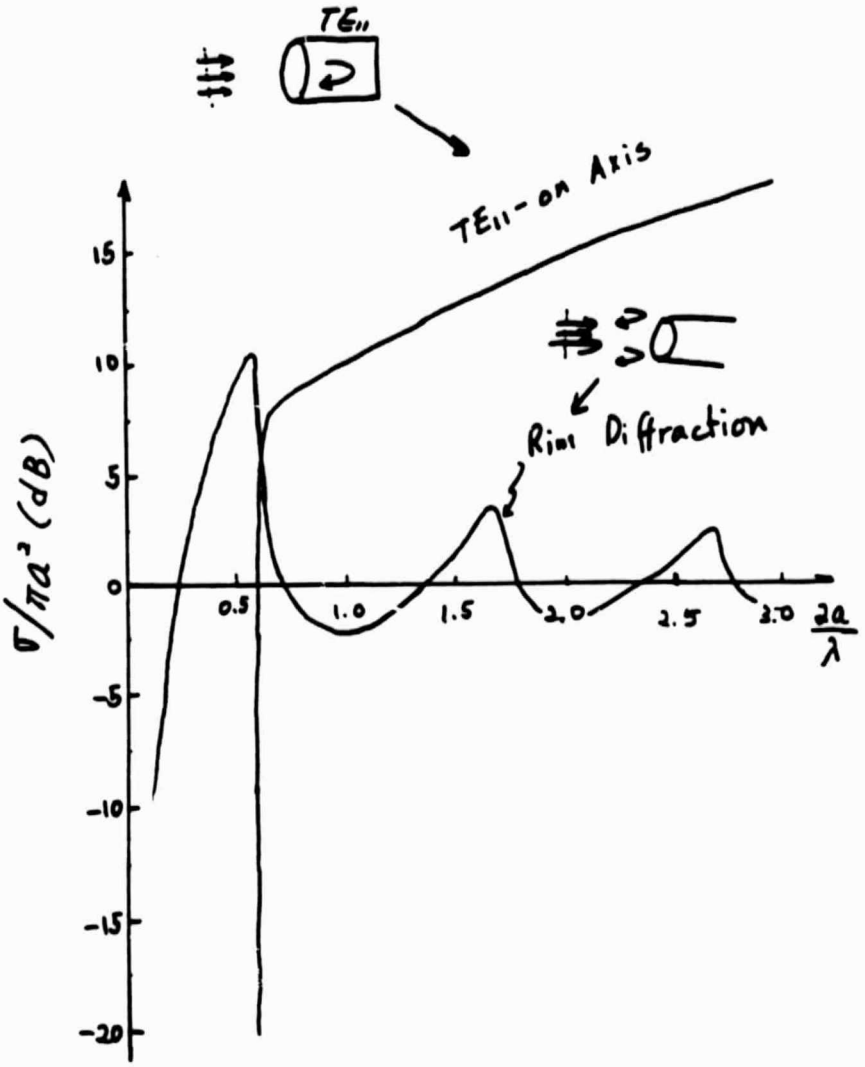

Figure 20. The RCS's from the interior irradiation of the TE_{11} mode only and the rim diffraction of a circular waveguide terminated by a PEC for a normal incidence as a function of a/λ (Source: Johnson and Moffatt, 1980 [10]).

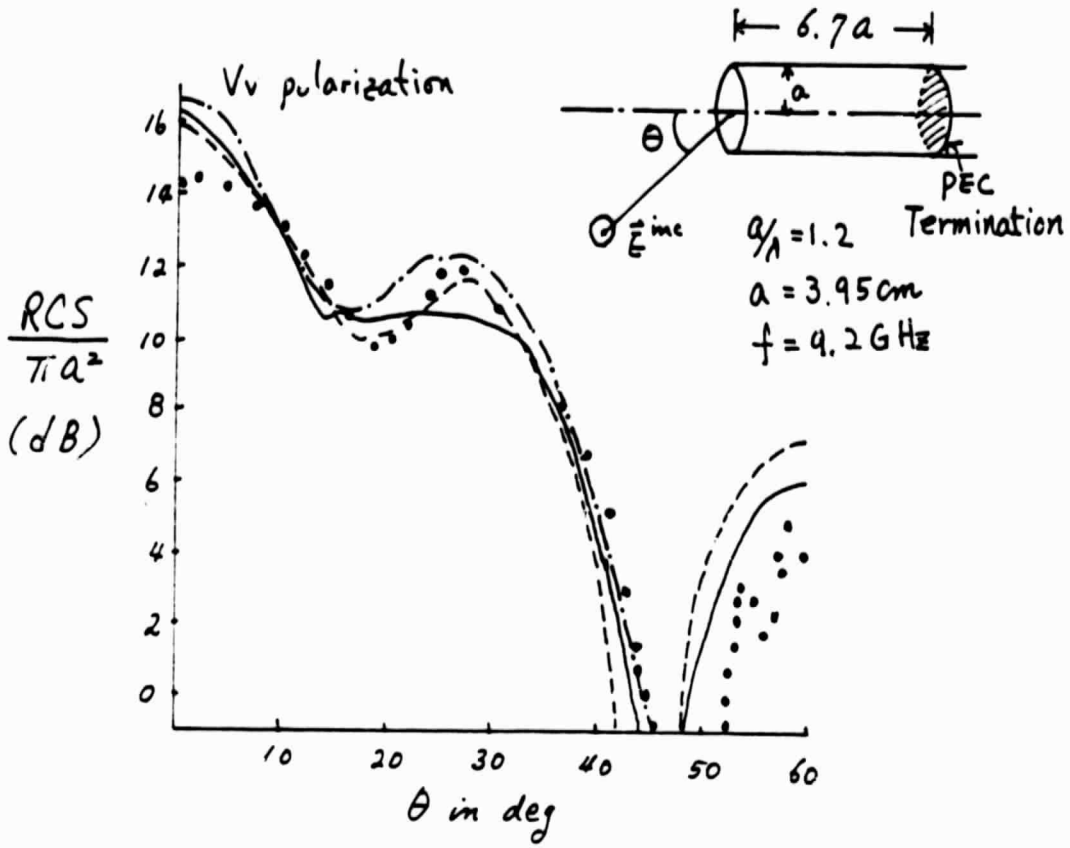

Author	Witt & Price	Mittra, Lee & Chuang	Our Solution	Witt & Price
Theory	Kirchhoff's + Rim Refl.	Wiener - Hopf	Kirchhoff's	Measure - ment
Year	1968	1974	1985	1968
Notation	- - - -	———	—·—·—·—	• • • •
Reference	[9]	[11]	—	[9]

Figure 21. The RCS from a circular waveguide terminated by a PEC in comparison with other solutions as a function of incident angle ($a/\lambda = 1.2$, length = 26.46 cm, a = 3.95 cm, vertical polarization).

Next we analyzed the contribution of each mode to the total RCS. Figure 22 shows the total RCS and the RCS's from a few normal modes in an uncoated circular waveguide terminated by a PEC, assuming all other modes except that particular mode are ignored. We see that the main peak near normal incidence is mainly due to the dominant TE_{11} mode. As discussed in Section 1, with a thin coating of a magnetic-material layer, the HE_{11} mode (which corresponds to the TE_{11} mode in an uncoated waveguide) can be eliminated and the RCS can be drastically reduced within a small angle, $\theta_0 = \tan^{-1} 1.84\ \lambda/(2\pi a)$.

For the calculation of the RCS, consider the cylindrical waveguide shown in Figure 14. The layer thickness increases gradually near the waveguide mouth. The reason for this is that for a normal mode to have a large attenuation constant, the field must be large around the small area of the lossy region. In other words, the mode similar to a surface mode has a large attenuation constant. If the layer thickness is uniform up to the waveguide mouth, this mode would not couple very much with the incident plane wave because the incident plane wave does not overlap much with the surface mode. For example, when the coating is tapered near the waveguide mouth (Figure 14), the dominant HE_{11} mode will be highly excited (~84% of the intercepted energy at normal incidence) at the waveguide opening, and then this will be transformed into a surface mode as it propagates through the gradually coated waveguide. All normal modes excited at the waveguide opening will be transmitted into the waveguide without reflection or modal conversion if the transition region is long enough [14]. It is not clear yet at this stage of our research how long the transition region must be. But we can conjecture from the result of the waveguide taper that the reflection at the low frequency can be minimal with a transition length of $\lambda/2$ in a well-designed taper [15]. At the higher frequency ($a/\lambda \gg 1$), the power reflected backward is much smaller than the power scattered

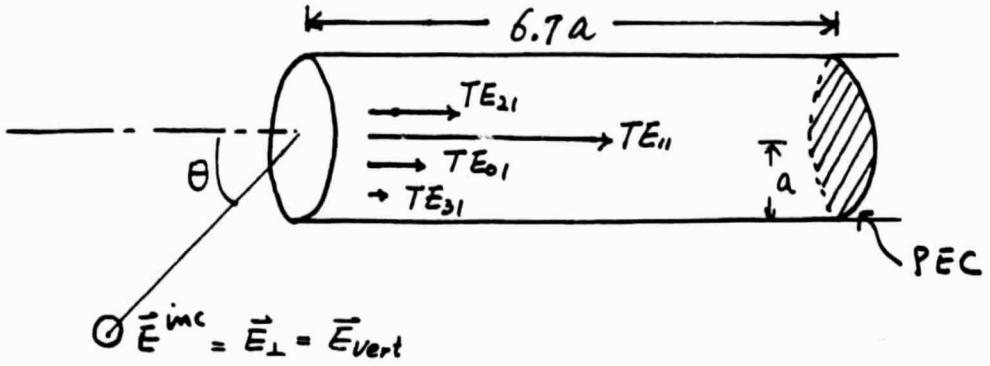

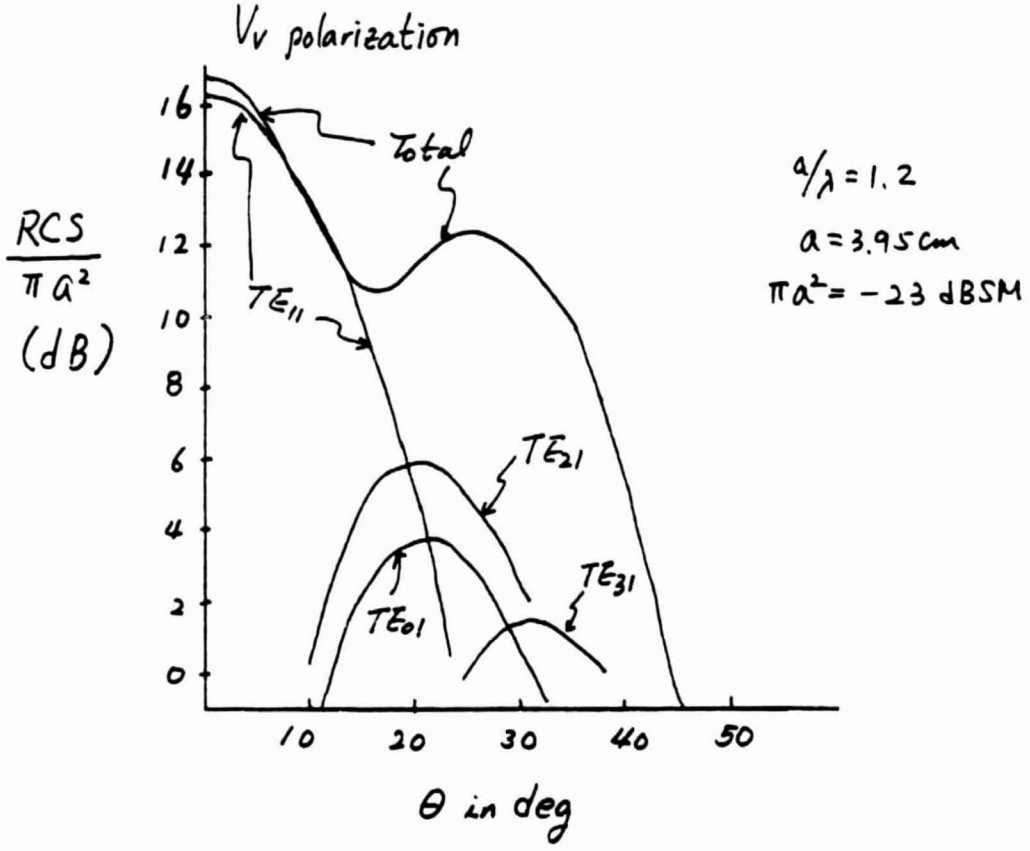

Figure 22. The total RCS and the RCS's from a few low-order modes in a circular waveguide terminated by a PEC (a/λ = 1.2, length = 26.46 cm, a = 3.95 cm, vertical polarizaton).

forward (modal conversion) and the transition region should be longer than that at the low frequency. In this report we assume that the transition distance is about $\lambda/2$ for the low-frequency case and a diameter distance for the intermediate- and high-frequency cases. The exact transition length is to be determined in the near future.

Since the normal modes in the transition region have not been analyzed yet, we approximate in this report that the phase change in the transition region is taken to be the value if a half of the transition region is coated uniformly and the other half is not coated (Figure 23), and all normal modes at the waveguide opening excited by an incident plane wave are completely transmitted into the waveguide without any reflection or modal conversion.

Now we consider the RCS at the low frequency ($a/\lambda = 1.2$). As indicated in Section 1, we chose a very lossy magnetic material for coating, that is, Crowley BX113 ($\varepsilon_r = 12 - j0.144$, $\mu_r = 1.74 - j3.306$) [16]. Figure 24 shows the power distribution of the HE_{11} mode for a few different thicknesses of the lossy layer. As discussed in Section 1, the power distribution does not change much with the layer thickness. In other words, the quasi-static approximation is valid and the transition region does not have to be long for a smooth transition of the normal modes. We assume that the transition length is about $\lambda/2$ in our RCS calculation. In this low-frequency case ($a/\lambda = 1.2$), 10 normal modes are excited by the incident plane wave for a vertical polarization. The attenuation constants of these normal modes are shown in Table 2 for two layer thicknesses. We note that all the modes have large attenuation constants and the modal separation (Table 2) is not apparent. Another two interesting points should be noted in Table 2. First, usually a higher-order mode has a larger attenuation constant than that of a lower-order mode, which is not the case for the dielectric coating. This is a good sign because the modal conversion (e.g.,

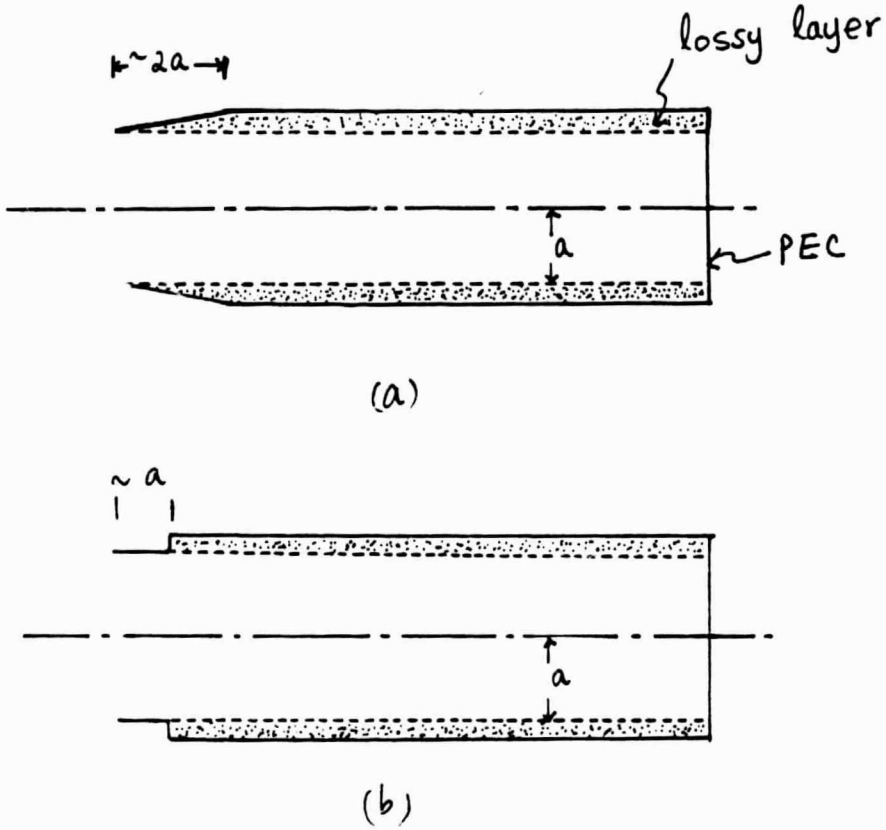

Figure 23. (a) The circular waveguide coated with a lossy material with a taper near the waveguide mouth. (b) The approximation of (a) in the calculation of the RCS in this report with an assumption that all normal modes are transmitted without reflection or modal conversion.

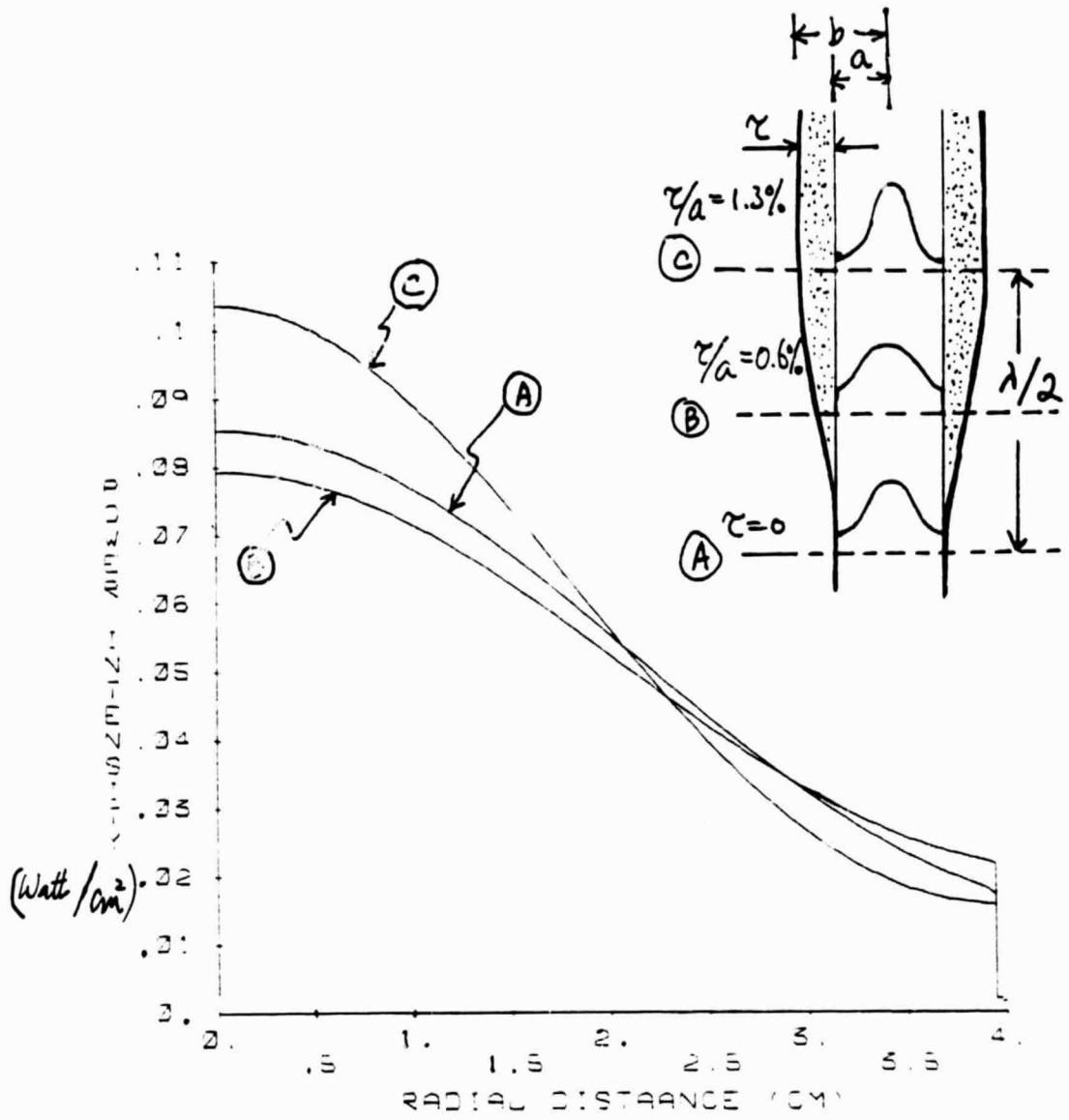

Figure 24. Power intensity of the HE_{11} mode as a function of the radial distance in a waveguide coated with a lossy material (Crowloy BX113, $\varepsilon_r = 12 - j0.144$, $\mu_r = 1.74 - j3.306$) with a total power of 1 watt: $f = 9.2$ GHz, $a = 3.95$ cm, A. $b = 3.95$ cm ($\tau = 0$ cm), B. $b = 3.975$ cm ($\tau = 0.025$ cm), and C. $b = 4.00$ cm ($\tau = 0.05$ cm).

TABLE 2.

ATTENUATION CONSTANTS OF THE NORMAL MODES IN A CIRCULAR WAVEGUIDE COATED WITH A LOSSY MATERIAL (CROWLOY BX113, $\varepsilon_r = 12 - j0.144$, $\mu_r = 1.74 - j3.306$) FOR 0.6% (a = 3.95 cm, $\tau = 0.025$ cm) AND 1.3% (a = 3.95 cm, $\tau = 0.05$ cm) COATINGS

Normal Modes	$\tau = 0.025$ cm (0.6% Coating)	$\tau = 0.05$ cm (1.3% Coating)
HE_{01}	−0.40	−0.84
HE_{02}	−2.80	−5.57
HE_{11}	−0.86	−1.35
HE_{12}	−1.00	−2.11
HE_{21}	−1.66	−3.41
HE_{22}	−2.43	−4.95
HE_{31}	−2.57	−5.64
HE_{41}	−3.82	−8.44
HE_{51}	−5.99	−12.79
HE_{61}	−12.33	−21.20

from a dominant mode to a higher-order mode) would not be critical in this case. Second, the attenuation constant of a normal mode for the two-thickness layer is about twice as large. This indicates that the field distribution of a normal mode does not change much with the layer thickness, which we observed earlier in Figure 24. The result is a uniform reduction of the RCS over a wide incident angle (Figure 25). With the layer thickness of 0.6% of the radius, the overall RCS reduction is more than 10 dB, and with 1.3% coating the reduction is more than 18 dB, which brings down the RCS below the RCS from the rim diffraction of the waveguide (Figure 12).

Next we consider the RCS from the intermediate frequency ($a/\lambda = 3.3$). As indicated in Section 1, we need to choose less lossy magnetic material than that for the low frequency. The best material we can find is poly-2,5-dichlorostyrene ($\varepsilon_r = 7.3$, $\mu_r = 9.1 - j0.32$)[16]. Figure 26 shows the power intensity of the HE_{11} mode as a function of the radial distance for a few different layer thicknesses. We note that the modal-field distribution shifts to the lossy layer as the layer thickness becomes larger and the attenuation constant becomes very large. On the other hand, the drastic change of the modal-field distribution with the layer thickness indicates that the transition region must be long in order to prevent the modal conversion from a highly attenuated mode to a lowly attenuated mode. Note that the HE_{11} would be an inner mode if the coating material is a more lossy magnetic material (e.g., Crowloy BX113). In order to prevent this modal separation, we chose a less lossy magnetic material. However, this less lossy material would not provide sufficient attenuation for the high-order modes, and a thicker lossy layer may be required to obtain a desired RCS reduction. Note that once the modal separation occurs, increasing the layer thickness would not help much to reduce the RCS. Table 3 shows the attenuation constants of the normal modes excited by an

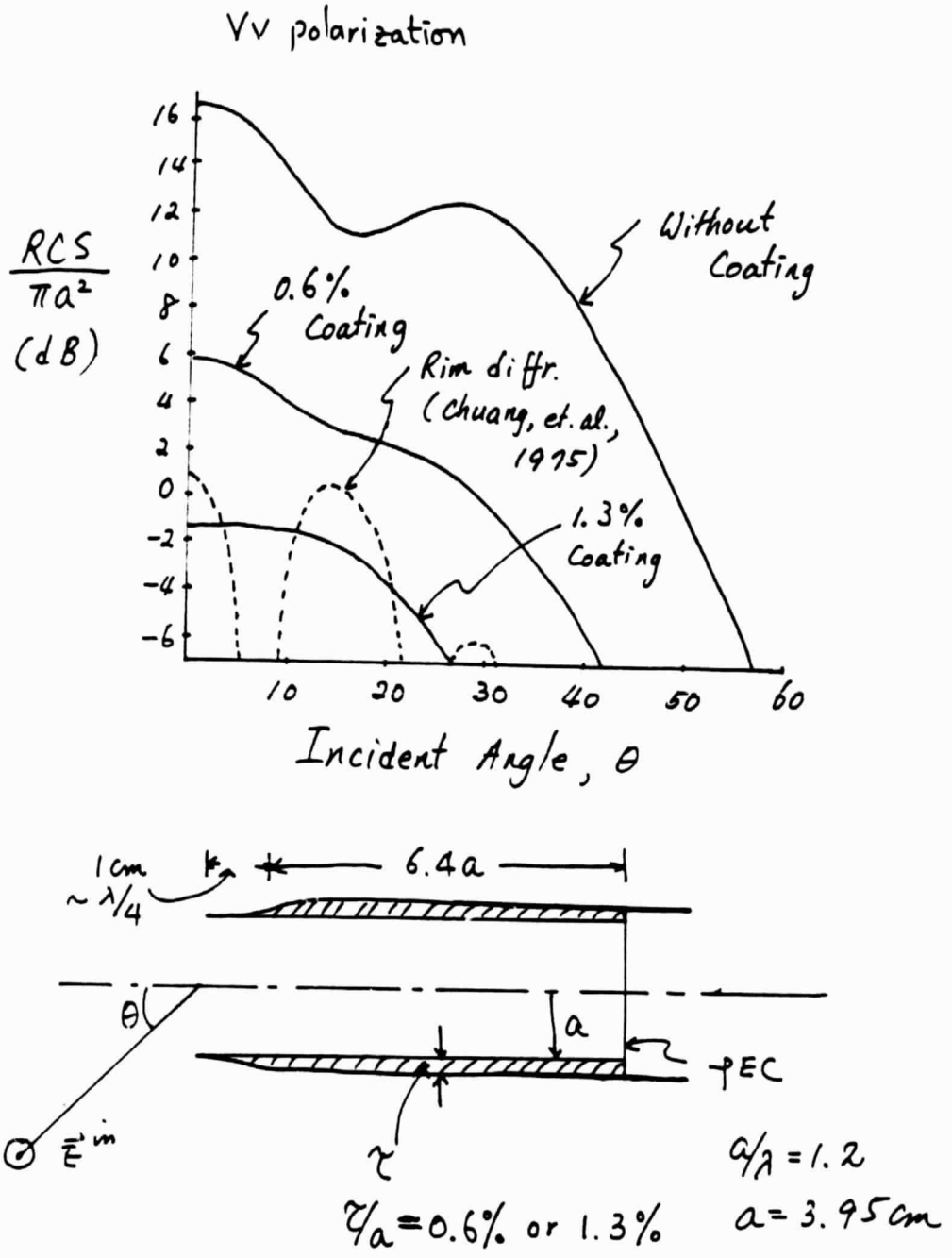

Figure 25. The RCS's as a function of the incident angle from a circular waveguide coated with a lossy material (Crowloy BX113, $\varepsilon_r = 12 - j0.144$, $\mu_r = 1.74 - j3.306$) and terminated by a PEC for layer thicknesses of $\tau = 0$, 0.025 cm (0.6% coating) and 0.05 cm (1.3% coating) (a = 3.95 cm, f = 9.2 GHz, a/λ = 1.2, length = 26.46 cm, vertical polarization).

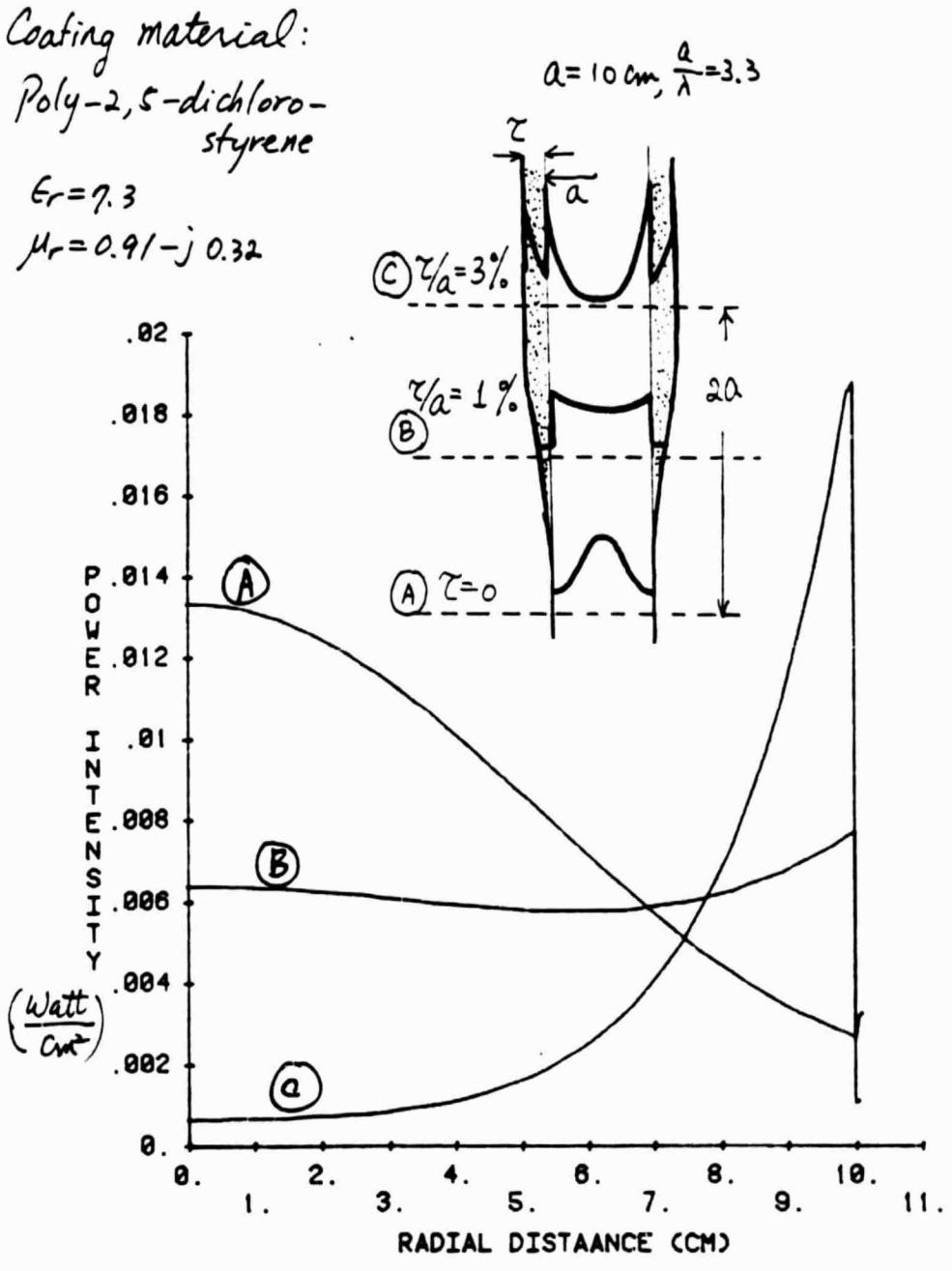

Figure 26. Power intensity of the HE_{11} mode as a function of the radial distance in a waveguide coated with a lossy material (Poly-2,5-dichlorostyrene, $\varepsilon_r = 7.3$, $\mu_r = 9.1 - j0.32$) with a total power of 1 watt: f = 10 GHz, a = 10 cm, A. b = 10 cm (τ = 0 cm), B. b = 10.1 cm (τ = 0.1 cm), and C. 10.3 cm (τ = 0.3 cm).

TABLE 3.

ATTENUATION CONSTANTS OF THE NORMAL MODES IN A CIRCULAR WAVEGUIDE COATED WITH A LOSSY MATERIAL(POLY-2,5-DICHLOROSTYRENE, $\varepsilon_r = 7.3$, $\mu_r = 9.1 - j0.32$) FOR 1% (a = 10 cm, τ = 0.1 cm) AND 3% (a = 10 cm, τ = 0.3 cm) COATINGS

Normal Modes	τ = 0.1 cm (1% coating)	τ = 0.3 cm (3% coating)	Normal Modes	τ = 0.1 cm (1% coating)	τ = 0.3 cm (3% coating)
HE_{11}	-2.13	—*	HE_{13}	-1.32×10^{-1}	-1.62
HE_{21}	-2.19	—	HE_{23}	-2.03×10^{-1}	-2.41
HE_{31}	-2.32	—	HE_{33}	-2.89×10^{-1}	-3.30
HE_{41}	-2.48	—	HE_{43}	-3.93×10^{-1}	-4.43
HE_{51}	-2.66	—	HE_{53}	-5.19×10^{-1}	-5.75
HE_{61}	-2.86	—	HE_{63}	-6.77×10^{-1}	-7.45
HE_{71}	-3.08	—	HE_{73}	-8.82×10^{-1}	-9.58
HE_{81}	-3.31	—	HE_{83}	-1.17	-25.65
HE_{91}	-3.58	—	HE_{93}	-1.64	-12.93
HE_{101}	-3.87	—	HE_{103}	-1.64	-11.97
HE_{111}	-4.21	—			
HE_{121}	-4.59	—	HE_{33}	-1.81×10^{-1}	-3.87
HE_{131}	-5.06	—			
HE_{141}	-5.62	—	HE_{14}	-2.58×10^{-1}	-2.87
HE_{151}	-6.33	—	HE_{24}	-3.58×10^{-1}	-9.53
HE_{161}	-7.28	—	HE_{34}	-4.86×10^{-1}	-12.57
HE_{171}	-8.07	—	HE_{44}	-6.55×10^{-1}	-22.26
HE_{181}	-11.00	—	HE_{54}	-8.90×10^{-1}	-21.86
			HE_{64}	-1.26	-13.11
HE_{01}	-2.30×10^{-2}	3.99×10^{-1}	HE_{74}	-2.04	-14.16
HE_{21}	-6.82×10^{-2}	-9.01×10^{-1}			
HE_{22}	-1.35×10^{-1}	-9.51×10^{-1}	HE_{04}	-3.50×10^{-1}	-10.80
HE_{32}	-2.12×10^{-1}	-1.38			
HE_{42}	-3.00×10^{-1}	-1.91	HE_{15}	-4.78×10^{-1}	-20.82
HE_{52}	-3.99×10^{-1}	-2.55	HE_{25}	-6.56×10^{-1}	-20.92
HE_{62}	-5.13×10^{-1}	-3.33	HE_{35}	-9.21×10^{-1}	-12.67
HE_{72}	-6.44×10^{-1}	-4.28	HE_{45}	-1.39	-12.92
HE_{82}	-7.99×10^{-1}	-5.44	HE_{55}	-2.87	-14.69
HE_{92}	-9.88×10^{-1}	-6.89	HE_{65}	-6.58×10^{-1}	-20.04
HE_{102}	-1.23	-8.74			
HE_{112}	-1.55	-11.20	HE_{16}	-9.43×10^{-1}	-12.38
HE_{122}	-2.05	-14.59	HE_{26}	-1.51	-12.92
HE_{132}	-2.99	-19.43	HE_{06}	-1.55	-12.94
HE_{02}	-8.04×10^{-2}	-1.72			

* — indicates the attenuation is more than 100 dB down.

ORIGINAL PAGE IS OF POOR QUALITY

incident plane wave at the intermediate frequency ($a/\lambda = 3.33$). Note that the HE_{m1} ($m = 1,2,\ldots$) modes acquire large attenuation constants with a much thinner lossy layer than other high-order modes. The result is that the RCS reduction is not as uniform as that for the low-frequency case (Figure 27). However, with a somewhat thicker lossy layer than that for the low-frequency case, considerable RCS reduction can be achieved. It is interesting to note that the RCS peak from an uncoated waveguide near the normal incidence is mainly due to the HE_{11} mode (Figure 22), and that the HE_{11} mode has a larger attenuation constant with a very thin layer of coating (Table 3). Thus, an extremely thin lossy layer may be sufficient in order to reduce the RCS for a small incident angle.

Finally, we consider the high-frequency case ($a/\lambda = 13.3$). We first encounter a computational problem. The number of modes excited in this case is more than 1000 for the vertical polarization and 2000 for the horizontal polarization. Thus, we have calculated the RCS for the normal incidence only. The best macerial we can choose is the same as that for the intermediate frequency. First note a rapid change of the power distribution of the HE_{11} mode with the layer thickness, which indicates that the attenuation constant increases very rapidly with the layer thickness (Figure 28). The result is that the RCS for the normal incidence is reduced very rapidly as the layer thickness increases because the main contribution of the RCS at the normal incidence comes from the HE_{11} mode (Figure 29). Note that with less than 0.2% coating, the RCS is reduced by more than 20 dB. But this reduction is limited to a small incident angle ($\lesssim 1°$). The RCS reduction over a wide angle requires a thicker lossy layer.

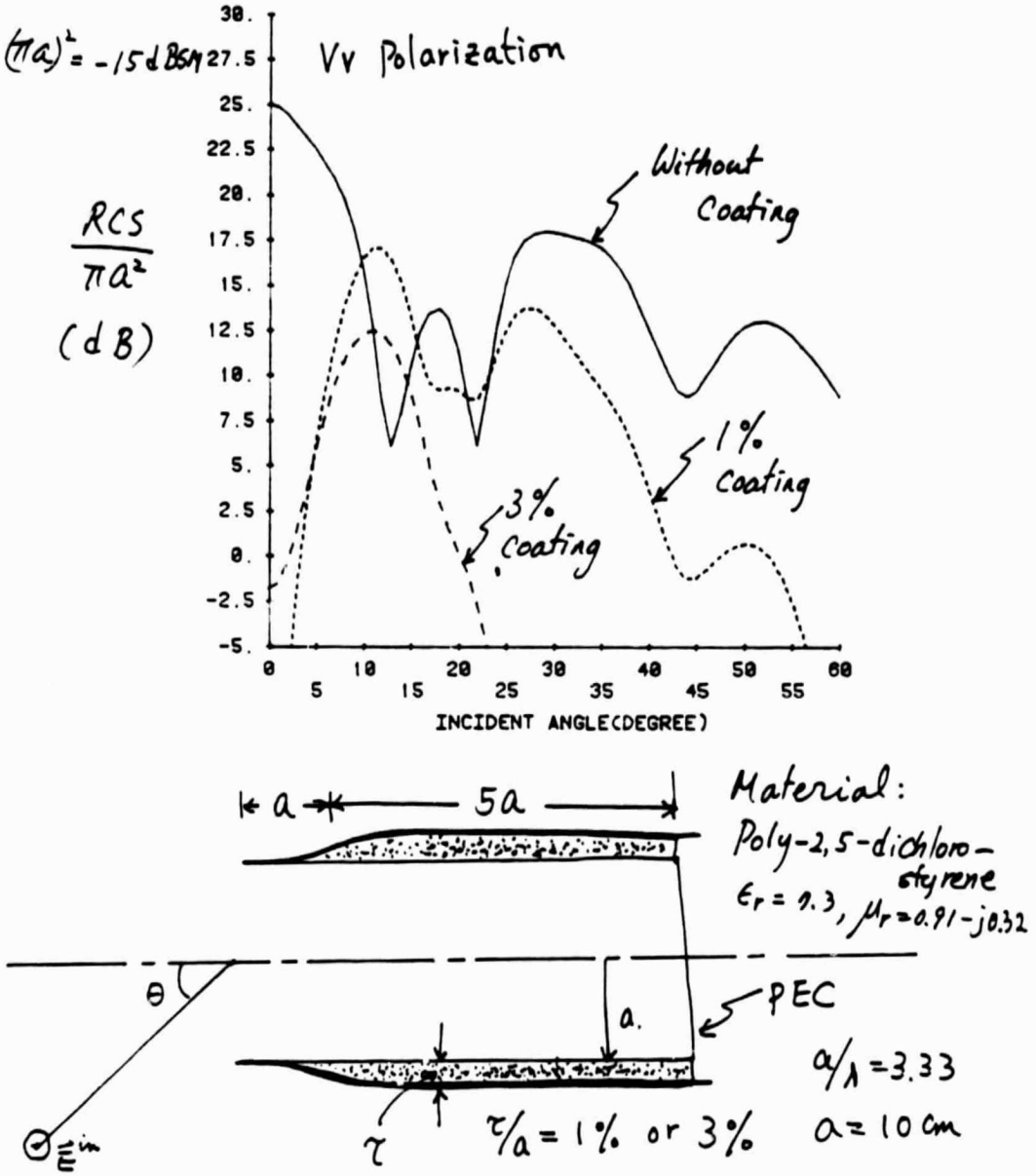

Figure 27. The RCS's as a function of the incident angle from a circular waveguide coated with a lossy material (poly-2,5-dichlorostyrene, $\varepsilon_r = 7.3$, $\mu_r = 9.1 - j0.32$) and terminated by a PEC for layer thicknesses of $\tau = 0$, 0.1 cm (1% coating) and 0.3 cm (3% coating) ($a = 10$ cm, $f = 10$ GHz, $a/\lambda = 3.33$, length = 60 cm, vertical polarization).

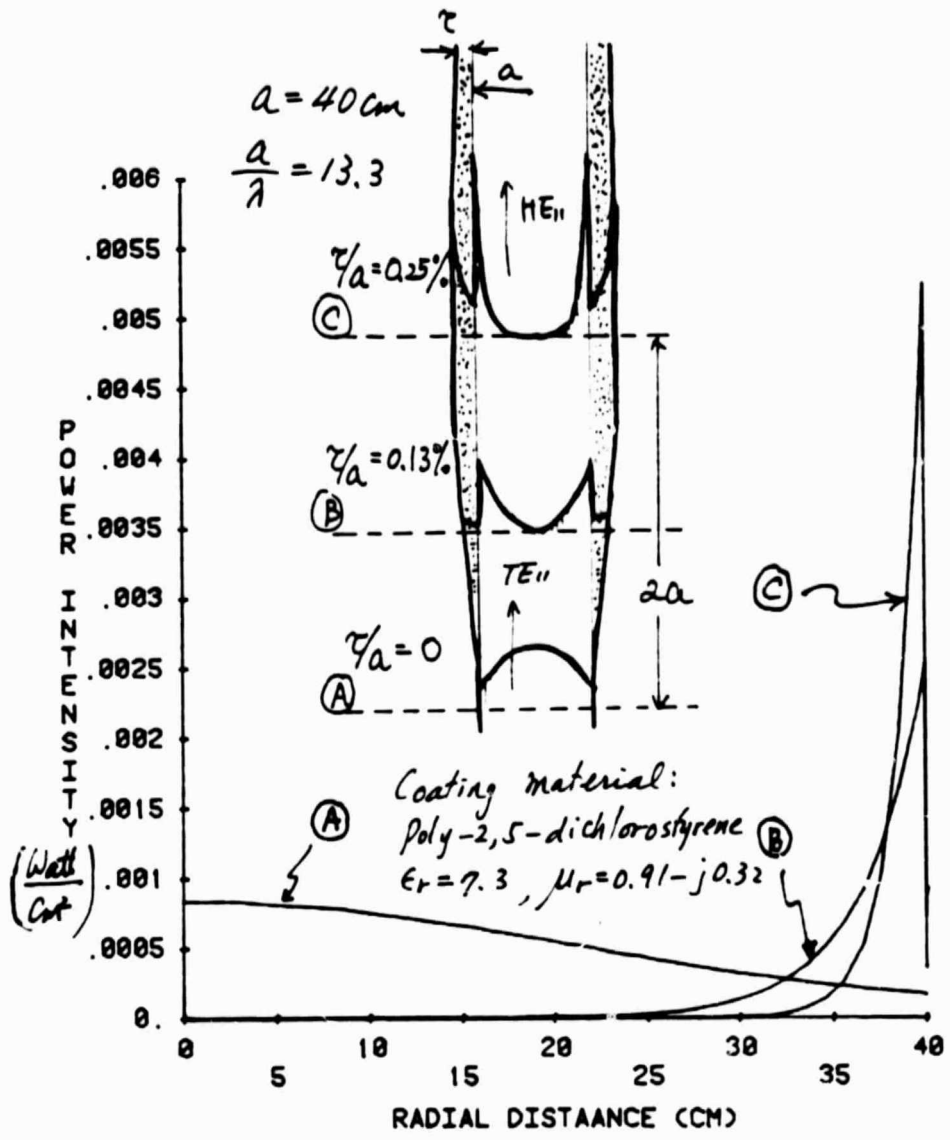

Figure 28. Power intensity of the HE_{11} mode as a function of the radial distance in a waveguide coated with a lossy material (poly-2,5-dichlorostyrene, $\varepsilon_r = 7.3$, $\mu_r = 9.1 - j0.32$) with a total power of 1 watt: f = 10 GHz, a = 40 cm, A. b = 40 (τ = 0 cm), B. b = 40.1 cm (τ = 0.1 cm), and C. b = 40.2 cm (τ = 0.2 cm).

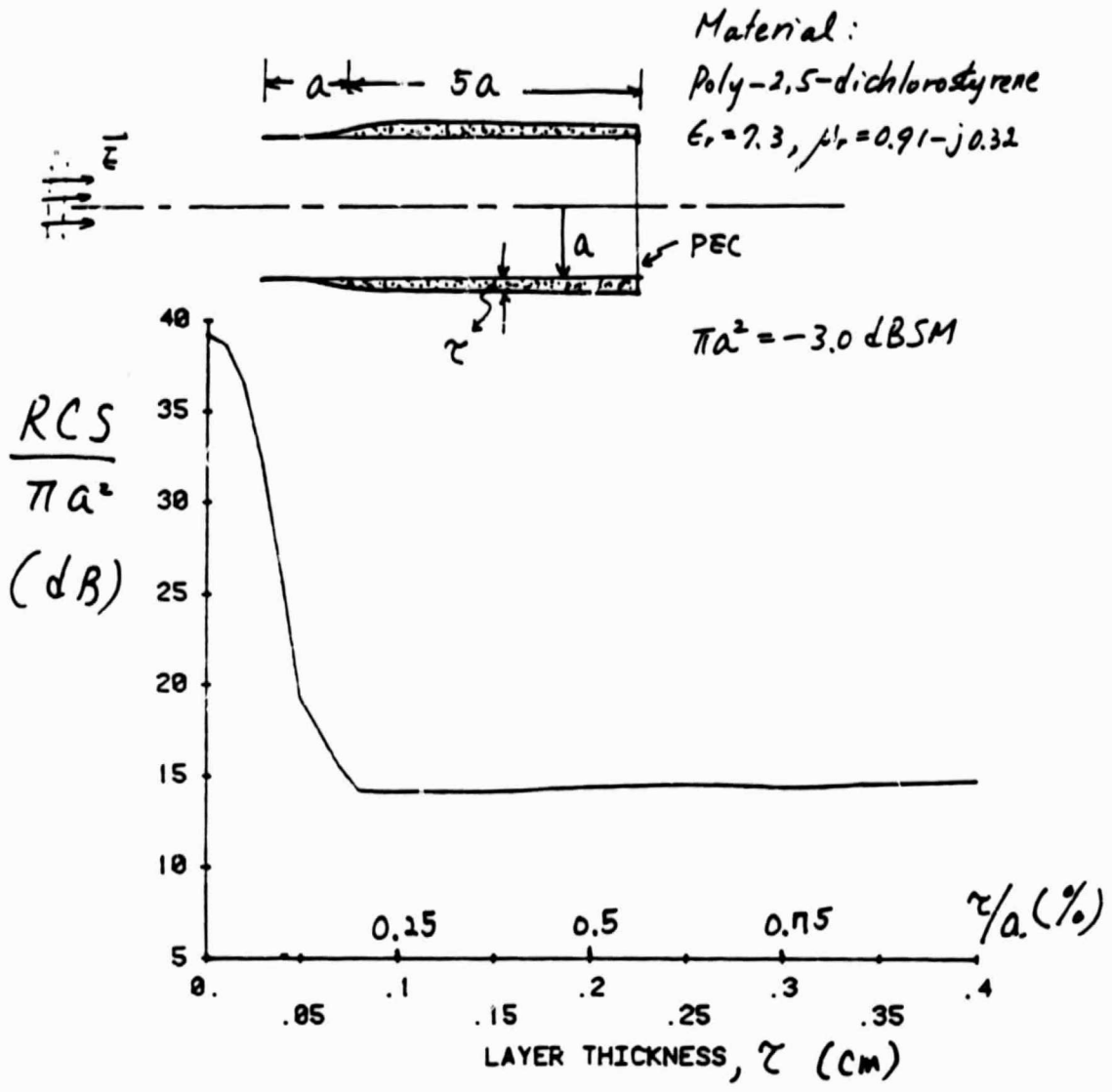

Figure 29. The RCS's as a function of the layer thickness from a circular waveguide coated with a lossy material (poly-2,5-dichlorostyrene, $\epsilon_r = 7.3$, $\mu_r = 9.1 - j0.32$) and terminated by a PEC (a = 40 cm, f = 10 GHz, $a/\lambda = 13.3$, length = 240 cm, vertical polarization).

(3) A by-product of our research: A waveguide coated with a very lossy magnetic material as a substitute of a corrugated waveguide

To produce a circularly polarized field, the open-ended corrugated waveguide is one of the most popular choices [17] - [20]. The dominant HE_{11} mode in a corrugated waveguide approximately satisfies the following boundary conditions at the waveguide wall:

$$E_\phi = 0 \quad \text{and} \quad H_\phi = 0$$

where E_ϕ and H_ϕ are the angular components of the electric and magnetic fields, respectively. These conditions are the requirements for producing a good circularly polarized field [17]. In this section we will show that the above boundary conditions can be approximately met by the HE_{11} mode in a smooth-walled circular waveguide coated with a thin layer of lossy magnetic material. In order that the above boundary conditions are to be reasonably satisfied, the coating material must be sufficiently lossy and the diameter of the waveguide must be significantly larger than the free-space wavelength.

Figure 30 shows the magnitudes of the angular components of the fields at the interface between the air and the lossy material relative to those at the center of the waveguide. The fields are reduced significantly by increasing the radius of the waveguide. Similarly, the attenuation constant decreases very rapidly as the radius of the waveguide increases (Figure 31). In the high-frequency limit ($ka \gg 1$), the attenuation constant is proportional to $1/(k^2a^3)$ where $k = 2\pi/\lambda$ and a is the inner radius of the waveguide. (A similar result has been obtained for the EH_{11} mode in a hollow dielectric waveguide [7].) Thus the loss in the magnetic material can be made reasonably small by choosing a large waveguide with a relatively high operating frequency, e.g., in the millimeter-frequency regime.

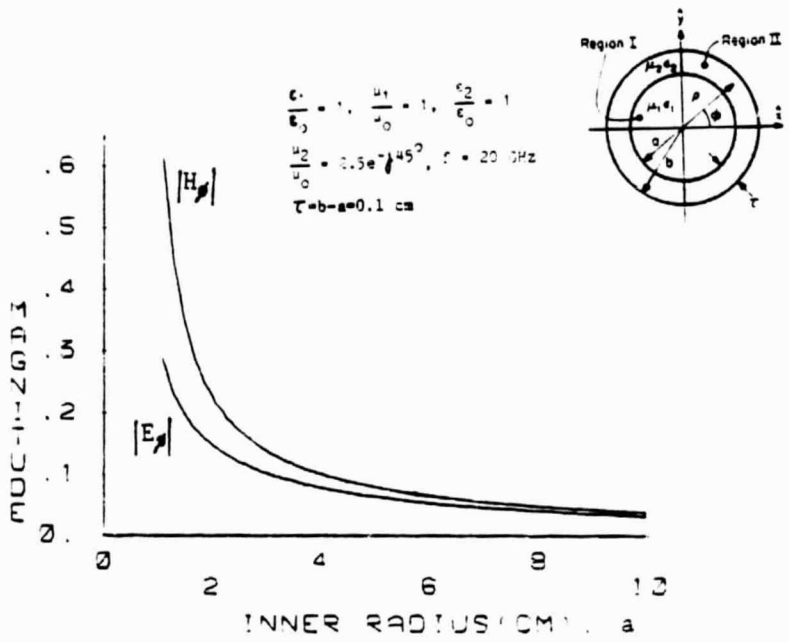

Figure 30. The magnitudes of the angular electric and magnetic fields of the HE_{11} mode at the interface between the air and the lossy material relative to those at the center of the waveguide as a function of the inner radius of the waveguide, a(τ = 0.1 cm).

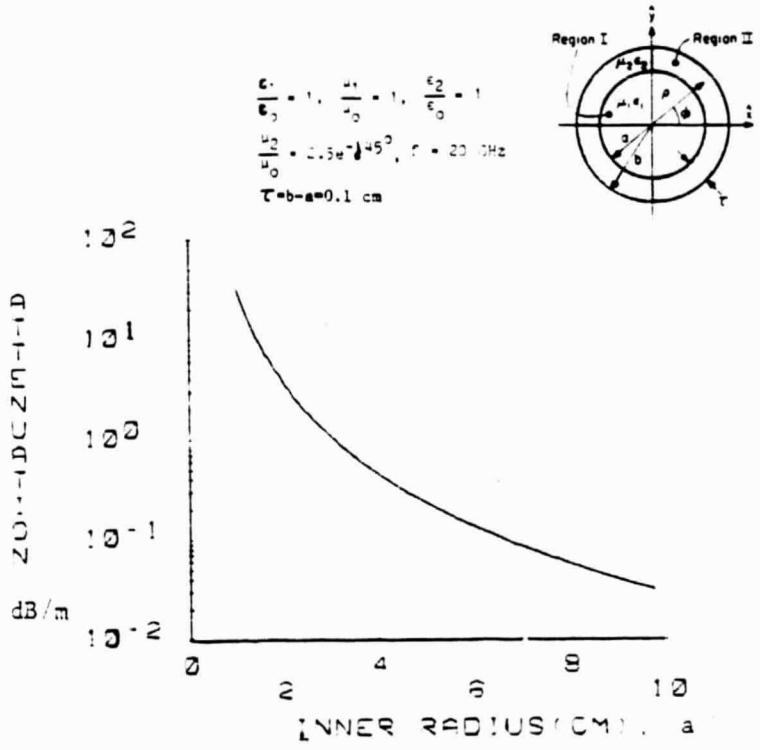

Figure 31. The attenuation of the HE_{11} mode as a function of the inner radius of the waveguide, a (τ = 0.1 cm).

The far-field radiation patterns in E and H planes from the HE_{11} mode in the open-ended waveguide coated with a lossy magnetic material are obtained by using the Kirchhoff-Huygen approximation (Figures 32a, 33, and 34). In Figure 32a the radius of the waveguide is relatively large ($a/\lambda = 6.67$), and we observe very low attenuation and negligible cross-polarization down to -50 dB. The beamwidth $2\theta_1$ is given by

$$(ka) \sin \theta_1 = 2.05$$

and the side-lobe level is -27.6 dB. These values agree well with the theoretical calculation for an ideal circular waveguide assuming the tangential fields vanish at the waveguide wall [20]. For the purpose of comparison, the radiation patterns from the TE_{11} mode in an empty open-ended waveguide are also shown (Figure 32b). In Figure 33, the radius is a half of that in Figure 32a, and the cross-polarization is still small down to -35 dB, but the attenuation is eight times larger than that in Figure 32a. Finally in Figure 34, the radius is close to the free-space wavelength ($a/\lambda = 1.33$), and we notice very large attenuation and appreciable cross-polarization.

Even though the attenuation of the HE_{11} mode in the waveguide coated with a lossy magnetic material may be larger than that of a well-designed corrugated waveguide, this waveguide as a microwave-feed device has two advantages over the corrugated waveguide:

1) less expensive to be built, and

2) having a wider operating-frequency range.

In a practical design, one must compromise between the dimension of the waveguide and the attenuation or cross-polarization level.

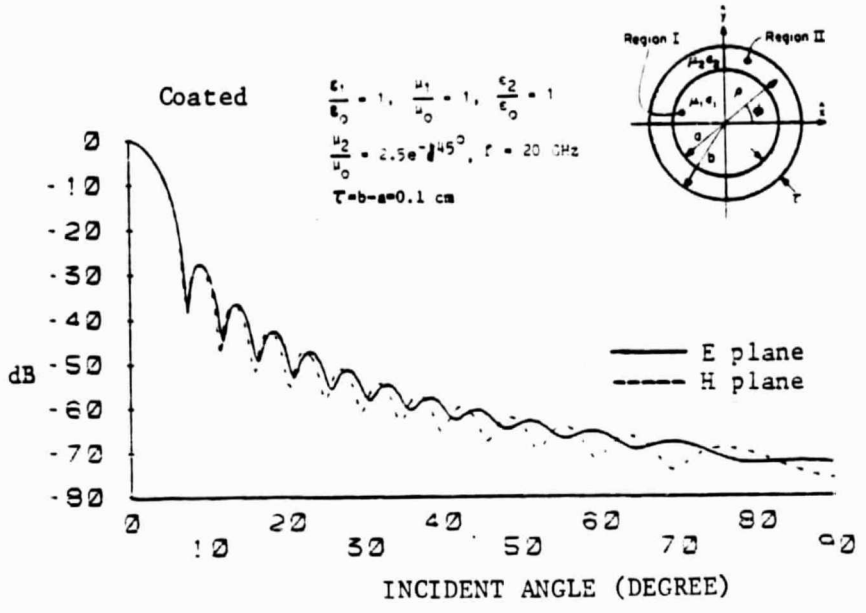

(a)

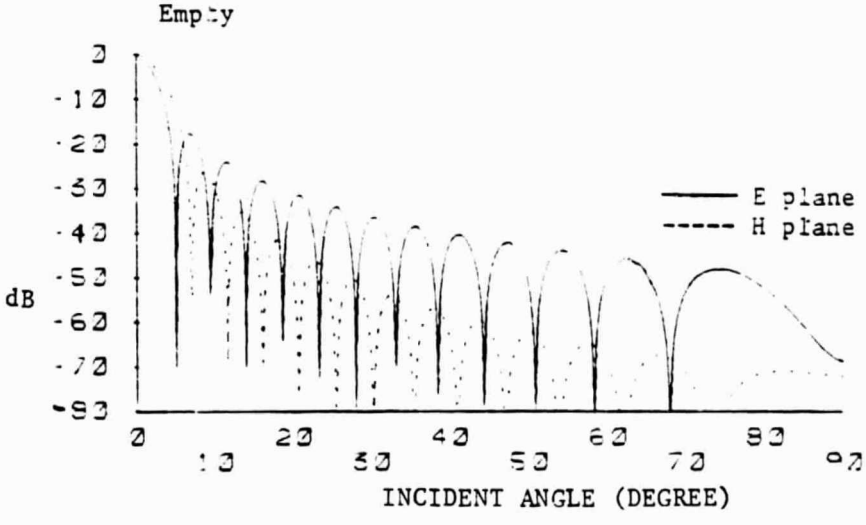

(b)

Figure 32. (a) The far-field radiation patterns of the HE_{11} mode in a coated guide: a = 10 cm, b = 10.1 cm, $a/\lambda = 6.67$. Loss = 2.84×10^{-2} dB/m. (b) The far-field radiation patterns of the TE_{11} mode in an empty guide: a = b = 10 cm, $a/\lambda = 6.67$.

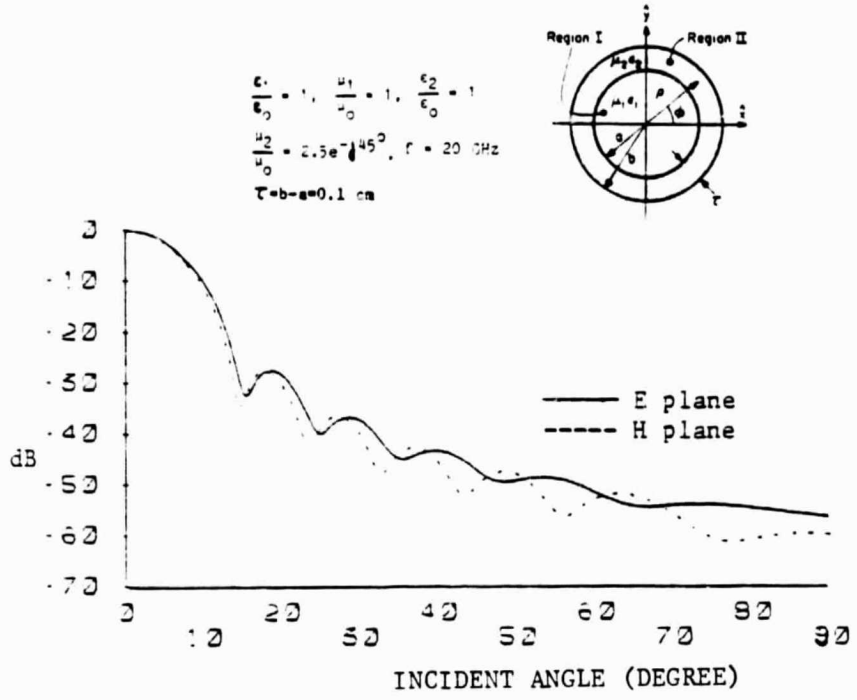

Figure 33. The far-field radiation patterns of the HE_{11} mode in a coated guide: a = 5 cm, b = 5.1 cm, $a/\lambda = 3.33$. Loss = 2.28×10^{-1} dB/m.

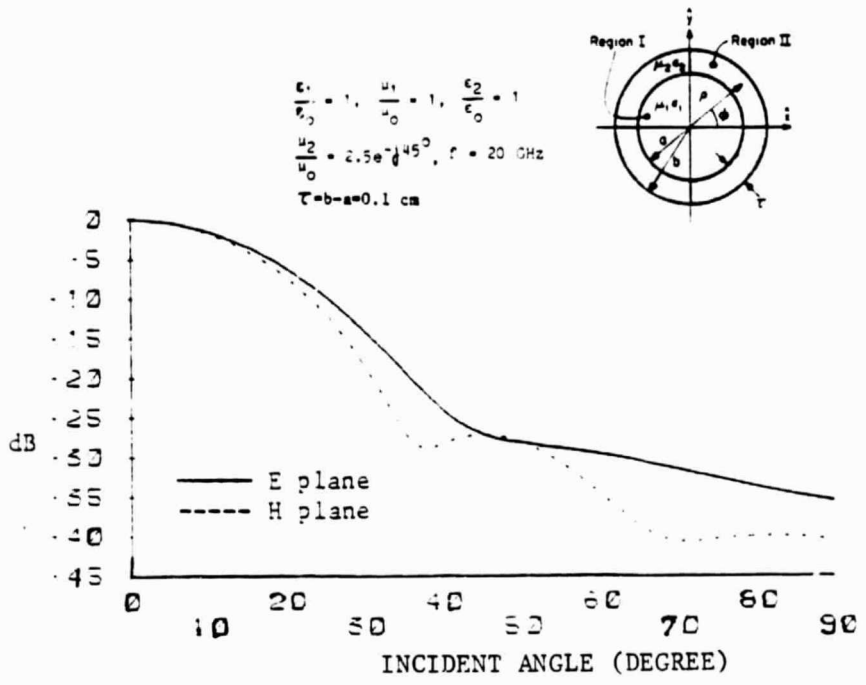

Figure 34. The far-field radiation patterns of the HE_{11} mode in a coated guide: a = 2 cm, b = 2.1 cm, $a/\lambda = 1.33$, Loss = 3.72 dB/m.

(4) Conclusions and future prospects

(i) We have shown that the interior irradiation from a circular waveguide terminated by a PEC contributes to the RCS much more than the rim diffraction, especially at high frequency (more than 10 dB for $a/\lambda \gtrsim 1$).

(ii) As indicated in the previous report [1], a very lossy magnetic material is suggested for coating at low frequency ($a/\lambda \sim 1$). Using the best material available with a layer thickness less than 1% of the radius, the RCS from a 7a-long circular waveguide ($a/\lambda = 1.2$) terminated by a PEC can be reduced more than 10 dB down over a broad incident angle.

(iii) At high frequency ($a/\lambda > 3$), the modal separation between the highly attenuated and the lowly attenuated modes occurs if the coating material is too lossy. This is not desirable in the application of the RCS reduction because the unattenuated normal modes will cause a large RCS in a certain incident angle. With the modal separation, increasing the layer thickness would not help to reduce the RCS because the attenuation constants of the normal modes do not change much with the layer thickness in this limit. Therefore, at the high frequency, the coating material must be less lossy than that at the low frequency.

Using the somewhat less lossy material for coating, some high-order modes do not attenuate much and a much thicker layer is required for those modes to attenuate considerably. However, the dominant mode acquires a large attenuation constant with a very thin layer of coating. Since the RCS for a small incident angle is mainly due to

the dominant mode, a very thin coating is required when the incident angle is small. For example, the RCS from a cylindrical waveguide ($a/\lambda = 13.3$, length = 6a, a = 10 cm) terminated by a PEC is reduced more than 20 dB down over the incident angle less than 1° when the layer thickness is less than 0.2% of the radius, using the best material available for coating.

(iv) Since the "effective" thickness of coating depends on $|\varepsilon_r \mu_r|$ of the lossy material, the layer thickness for a significant RCS reduction can be reduced by choosing a material with large $|\varepsilon_r \mu_r|$.

(v) From this study, it may be possible to reduce the RCS from a cylindrical waveguide terminated by a PEC considerably with a reasonable thickness of the coating. However, the optimal coating material strongly depends on the frequency and the radius of the waveguide. Thus the single-layer coating may be effective only over a certain range of frequency.

We have seen that the dielectric and the magnetic coatings provide distinctive properties of the normal modes in the waveguide. Combining these two characteristics through a multi-layer structure, it may be possible to provide a large RCS reduction over a wide frequency range. This possibility is under study.

(vi) We have shown that the layer thickness must be gradual near the waveguide opening. Though much work has been done on the taper-waveguide problem [14], our problem at the transition region appears to be new. We are planning a further research on this topic.

(vii) So far our research has been limited to a ciruclar waveguide. In the future, we are going to expand our project to include the problem of

a waveguide with an arbitrary cross section. The process to implement the finite-element method for this problem is in progress.

(viii) Finally, we are planning to do some experiments to verify some of our results.

REFERENCES

[1] S. W. Lee, Y. T. Lo, and S. L. Chuang, "Numerical Methods for Analyzing Electromagnetic Scattering," Semiannual Report to NASA Lewis Research Center, Cleveland, Ohio, September 1984.

[2] K. Suetake, Y. Kotsuka, K. Ishino, and Y. Hashimoto, "Microwave Applications of Thin Magnetic Resistive Sheets," 1977 International Microwave Symposium Digest, San Diego, 21-23 June 1977.

[3] Y. Kotsuka, "Microwave Simple Coaxial Attenuator Using Rubber Ferrite," Ferrites, Proceedings of the International Conference, September-October 1980, Japan.

[4] J. W. Carlin and P. D'Agostino, "Low-loss Modes in Dielectric Lined Waveguide," Bell System Tech. J., Vol. 50, pp. 1631-1638, May-June 1970.

[5] J. W. Carlin and P. D'Agostino, "Normal Modes in Overmoded Dielectric-Lined Circular Waveguide," Bell System Tech. J., Vol. 52, pp. 453-486, April 1973.

[6] P. J. B. Clarricoats, A. M. B. Al-Haviri, A. D. Olver, and K. B. Chan, "Low-attenuation Characteristics of Dielectric-Lined Waveguide," Electronics Letters, Vol. 8, pp. 407-409, August 1972.

[7] E. A. J. Marcatili and R. A. Schmeltzer, "Hollow Metallic and Dielectric Waveguides for Long Distance Optical Transmission and Lasers," Bell System Tech. J., pp. 1783-1809, July 1964.

[8] S. W. Lee and L. Grun, "Radiation from Flanged Waveguide: Comparison of Solutions," IEEE Trans. Antennas Propagat., Vol. AP-30, pp. 147-148, January 1982.

[9] H. R. Witt and E. L. Price, "Scattering from Hollow Conducting Cylinders," Proc. IEE, Vol. 115, pp. 94-99, January 1968.

[10] T. W. Johnson and D. L. Moffatt, "Electromagnetic Scattering by an Open Circular Waveguide," The Ohio State Univ., ElectroScience Laboratory, Columbus, Ohio, Technical Report 710816-9, December 1980.

[11] R. Mittra, S. W. Lee, and C. A. Chuang, "Analytic Modeling of the Radar Scattering Characteristics of Aircraft," Univ. of Illinois Electromagnetics Laboratory, Urbana, Illinois, Scientific Report No. 74-1, January 1974.

[12] C. A. Chuang, C. S. Liang, and S. W. Lee, "High Frequency Scattering from an Open-ended Semi-infinite Cylinder," IEEE Trans. Antennas Propagat., Vol. AP-23, pp. 770-776, November 1975.

[13] S. W. Lee, Classnotes for EE 497on GTD, University of Illinois, Fall of 1984.

[14] H. Unger, "Circular Waveguide Taper of Improved Design," Bell System Tech. J., Vol. 37, pp. 899-912, July 1958.

[15] R. E. Collin, "The Optimum Tapered Transmission Line Matching Section," Proc. IRE, Vol. 44, pp. 539-548, April 1956.

[16] A. R. Von Hippel, ed., "Dielectric Materials and Applications," Cambridge, Massachusetts: Technology Press, MIT, 1954.

[17] M. J. Al-Hakkak and Y. T. Lo, "Circular Waveguides and Horns with Anisotropic and Corrugated Boundaries," Antenna Laboratory Report No. 73-3, University of Illinois, Urbana, Illinois, 1973.

[18] P. J. B. Clarricoats, A. D. Olver, and S. L. Chong, "Attenuation in Corrugated Circular Waveguide, Part 1. Theory," Proc. IEE, Vol. 122, no. 11, pp. 1173-1179, 1975.

[19] C. Dragone, "Reflection, Transmission and Mode Conversion in a Corrugated Feed," Bell Syst. Tech. J., Vol. 56, no. 6, pp. 835-867, 1977.

[20] C. Dragone, "Attenuation and Radiation Characteristics of the HE_{11} Mode," IEEE Trans. Microwave Theory Tech., Vol. MTT-28, no. 7, pp. 704-710, 1980.